Modifying bacterial flagellin to evade Nod-like Receptor CARD 4 recognition enhances protective immunity against *Salmonella*

Panagiotis Tourlomousis[1], **John A. Wright**[#1], **Alessandra S. Bittante**[#1], **Lee J. Hopkins**[1], **Steven J. Webster**[1], **Owain J. Bryant**[2], **Pietro Mastroeni**[1], **Duncan J. Maskell**[1,4], **Clare E. Bryant**[1,*]

[1]Department of Veterinary Medicine, University of Cambridge, Cambridge, CB3 0ES, United Kingdom

[2]Department of Pathology, University of Cambridge, Cambridge, CB2 1QP, United Kingdom

[#] These authors contributed equally to this work.

Abstract

Pattern recognition receptors (PRRs) expressed in antigen-presenting cells are thought to shape pathogen-specific immunity by inducing secretion of co-stimulatory cytokines during T-cell activation, yet data to support this notion *in vivo* is surprisingly scarce. Here we show that the cytosolic PRR Nod-like Receptor CARD 4 (NLRC4) suppresses, rather than facilitates, effector and memory CD4^{+} T-cell responses against *Salmonella* in mice. NLRC4 negatively regulates immunological memory by preventing delayed activation of the cytosolic PRR NLR pyrin domain 3 (NLRP3) that would otherwise amplify the production of cytokines important for the generation of Th1 immunity such as intereukin-18. Consistent with a role for NLRC4 in memory immunity, primary challenge with *Salmonella* expressing flagellin modified to largely evade NLRC4 recognition significantly increases protection against lethal re-challenge. This finding suggests flagellin modification to reduce NLRC4 activation enhances protective immunity which could have important implications for vaccine development against flagellated microbial pathogens.

Antigen presenting cells (APCs) recognize pathogens via pattern recognition receptors (PRRs), such as the transmembrane Toll-like receptors (TLRs) and the cytosolic Nucleotide oligomerisation domain (NOD)-like receptors (NLRs)[1,2]. PRR activation induces APCs to secrete pro-inflammatory cytokines during presentation of antigens to naïve T cells leading to their differentiation into the most appropriate subset of activated T cells to eliminate the pathogen[3]. The bridge between the innate and adaptive immune systems is, therefore, formed by PRR activation in APCs. Central to this is the concept that the repertoire of PRRs

expressed by APCs is crucial to the specificity of adaptive immune response generated[4]. The increasing prevalence of antimicrobial resistance means the development of alternative ways to combat infectious diseases is a matter of urgency. Understanding the interactions between pathogens, PRRs and pathogen-specific immunity is, therefore, important to facilitate the development of new vaccines with improved efficacy.

Microbial pathogens produce a number of pathogen-associated molecular patterns (PAMPs) that are recognized by different PRRs. Lipopolysaccharide (LPS) from Gram-negative bacteria, for example, is recognized by TLR4 and flagellin by TLR5. Both flagellin and detoxified LPS molecules are used as vaccine adjuvants with flagellin being an antigenic target of antibody and CD4^{+} T cell responses[5]. The nucleotide binding oligomerisation domain (NOD)-like receptor CARD 4 (NLRC4) also recognizes microbial flagellin[6,7], but, in addition, senses the type III secretion system-associated needle and rod proteins[8] via the NLR family, apoptosis inhibitory protein (NAIP) 5 or NAIP6 and NAIP1 or NAIP2 in mice, respectively[9–11]. NLR pyrin domain 3 (NLRP3) is activated by a diverse range of triggers, including PAMPs and danger-associated molecular patterns (DAMPs). NLR activation drives the formation of an inflammasome signalling complex[12] which activates caspase-1 to process pro-IL-1β and pro-IL-18 to their mature forms and cleaves gasdermin D to drive an inflammatory form of cell death called pyroptosis[13,14]. NLRC4 and NLRP3 can be recruited to the same inflammasome to optimise IL-1β and IL-18 release[15,16].

IL-1β and IL-18 have well documented effects on T cell survival, activation and differentiation[17]. Little is known, however, about whether and how specific inflammasome components influence the development of adaptive immunity against pathogenic bacteria and, specifically, that of immunological memory which is critical for vaccine development[4]. It has been shown, for example, that NLRC4 and NLRP3 activation in innate immune cells optimises IFN-γ release by CD8+ and CD4^{+} T cells in mice challenged with *Salmonella enterica* serovar Typhimurium (*S.* Typhimurium), but this was not an antigen-specific effect[18,19]. Here, using the murine model of sublethal salmonellosis, we show that NLRC4 suppresses Th1 CD4^{+} T cell effector and memory responses against *S.* Typhimurium without affecting antibody production. Primary challenge with *S.* Typhimurium engineered to reduce NLRC4 inflammasome activation resulted in increased levels of serum IL-18 and IFN-γ, enhanced Th1 CD4^{+} T cell memory responses and improved protection against oral re-challenge with fully-virulent *Salmonella.* Our data suggest that attenuation of NLRC4 activation by flagellin could improve the efficacy of live vaccines against flagellated pathogens like *Salmonella,* and potentially that of flagellin-based adjuvants.

Results

NLRC4 restricts bacterial load *in vivo* and Th1 memory responses *ex vivo*

To investigate whether NLRC4 affects the development of pathogen-specific immunity, we first challenged C57BL/6J wild-type and congenic *Nlrc4*^{-/-} mice with *S.* Typhimurium M525P. In this model of sublethal salmonellosis, effector Th1 CD4^{+} T cells drive microbial clearance and establish long-term protection against re-challenge[20,21]. *Nlrc4*^{-/-} mice harboured higher microbial numbers in the liver and spleen irrespective of the route of bacterial administration (intravenous in Fig. 1a or oral in Extended Data 1a). Bacterial

burden, as expected [22,23], was not significantly different between $Nlrc4^{-/-}$ and wild-type mice lethally challenged with fully virulent *S.* Typhimurium SL1344 (Extended Data 1b). The slower kinetics of the sublethal infection reveal a clear role for NLRC4 in regulating bacterial load *in vivo*.

We determined whether NLRC4 would play any role in the development of memory CD4^{+} T cell responses. Wild-type and $Nlrc4^{-/-}$ mice were challenged with PBS (naïve) or 10^4 CFU of *S.* Typhimurium M525P, an inoculum size that was equally immunogenic to a 10-fold higher dose in wild-type mice (Extended Data 2) and well tolerated by the $Nlrc4^{-/-}$ mice. To elicit a response from memory cells only, CD4^{+} T cells were isolated from mice which had cleared the primary infection after a minimum of 90 days. Upon stimulation with bacterial extract (antigen-specific), CD4^{+} T cells from naïve mice, irrespective of genotype, secreted negligible amounts of the Th1 cytokines IFN-γ and IL-2 (Fig. 1b), confirming the specificity of the response generated by CD4^{+} T cells from infected mice (Fig. 1c). Similarly, the amount of IFN-γ secreted by CD4^{+} T cells when stimulated with anti-mouse CD3e (non antigen-specific) increased more than 50-fold in response to infection (Fig. 1c).

We compared the magnitude of the *ex vivo* memory responses between wild-type and $Nlrc4^{-/-}$ mice. T cells from $Nlrc4^{-/-}$ mice secreted more IFN-γ and IL-2 than cells from wild-type mice in response to both *Salmonella* antigen and anti-mouse CD3e (Fig. 1c). This amplified response persisted up to 170 days after challenge (Fig. 1d, concanavalin A was used in early experiments as a polyclonal stimulus but later replaced by anti-mouse CD3e). The Th1-related cytokines TNF-α, IL-6 and GM-CSF in the CD4^{+} T cell culture supernatant from $Nlrc4^{-/-}$ mice were also elevated (Fig. 1e). These data suggest that NLRC4 activation by *Salmonella* specifically restricts CD4^{+} T cell-mediated memory immunity.

We then quantified the number of CD4^{+} T-cells secreting IFN-γ in response to bacterial extract using ELISPOT and cytokine secretion assays. Both assays showed a larger population of IFN-γ-secreting cells in $Nlrc4^{-/-}$ mice (Fig. 1f and 1g). We also analysed the surface expression of CD62L and CD44 in IFN-γ+cells and found that over 90% in both wild-type and $Nlrc4^{-/-}$ mice had an effector memory T cell profile (CD44^{high} CD62L^{-}) with central memory cells (CD44^{high} CD62L+) representing less than 5% of the population (Extended Data 3). These data suggest that NLRC4 restricts T cell memory immunity against *Salmonella* by reducing the size of antigen-specific memory pool.

To test if NLRC4 could also affect protection against lethal re-challenge *in vivo*, wildtype and $Nlrc4^{-/-}$ mice were systemically challenged with *S.* Typhimurium M525P and, after clearing the primary infection, re-challenged orally with fully virulent *Salmonella. Nlrc4^{-/-}* mice were only marginally better protected than their wild-type counterparts (Extended Data 4b, mean survival time of 9 days versus 8 days, respectively), an outcome that may have been affected by the different routes of infection between primary challenge (intravenous) and re-challenge (orally). In the same trial, however, naïve $Nlrc4^{-/-}$ mice lethally challenged with *Salmonella* had shorter survival times than naïve wild-type mice (Extended Data 4a, 6 days versus 8 days, respectively). These data suggest that, in the absence of NLRC4, the compromised innate immune control of microbial dissemination presumably counteracts any benefits arising from augmented T-cell memory immunity.

NLRC4 restricts Th1 effector responses during microbial clearance of a primary infection

To determine if NLRC4 also affects the development of Th1 effector immunity, we isolated splenic CD4^{+} T cells from infected wild-type and *Nlrc4*^{-/-} mice during an active primary infection and measured the amount of IFN-γ released *ex vivo.* Production of IFN-γ in response to bacterial extract was comparable between the two genotypes when CD4^{+} T cells were isolated early during infection (Fig. 2a, 1 and 7 days). Notably, as the infection progressed into the phase of CD4^{+} T cell-mediated bacterial clearance, T cells from *Nlrc4*^{-/-} mice secreted significantly more IFN-γ than cells from wild-type mice (Fig. 2a, 14 and 21 days). By the end of microbial clearance, however, there were no difference in Th1 responses between *Nlrc4*^{-/-} and wild-type mice (Fig. 2a, 35 days). *Salmonella-induced* Th1 CD4^{+} T cell responses can also affect the development of B cell-dependent immunity[24], so we measured the levels of serum antibodies against *S.* Typhimurium LPS at 90 days after primary infection. We found no difference in the levels of IgG2c, IgG2b and IgM between wild-type and *Nlrc4*^{-/-} mice (Fig. 2b). These data collectively show that NLRC4 restricts both Th1 CD4^{+} T cell-mediated effector and memory immune responses against *Salmonella,* but has no effect on B cell-mediated immunity.

Negative regulation of CD4^{+} T cell-mediated memory responses by NLRC4 is NLRP3-dependent

NLRC4 is not expressed in naïve or activated CD4^{+} T cells[25,26]. We hypothesized, therefore, that any effect on CD4^{+} T cell memory immunity is most likely to occur in response to inflammasome signalling by APCs. NLRC4 and NLRP3 are both activated in murine macrophages infected with *Salmonella*[22]. We, therefore, assessed *ex vivo* the memory T cell responses in *Nlrp3*^{-/-} and *Nlrp3*^{-/-}*Nlrc4*^{-/-} mice. Secretion of both IFN-γ and IL-2 was comparable between wild-type, *Nlrp3*^{-/-} or *Nlrp3*^{-/-}*Nlrc4*^{-/-} mice (Fig. 3 a and 3b) and, as expected, we saw no difference in the numbers of CD4^{+} T cells secreting IFN-γ in response to bacterial extract (Fig. 3c and 3d). To confirm that our independent comparisons between wild-type and *Nlrc4*^{-/-} (Fig. 1c), wild-type and *Nlrp3*^{-/-} (Fig. 3a) and wild-type and *Nlrp3*^{-/-}*Nlrc4*^{-/-} mice (Fig. 3b) do not suffer from interexperimental variation, we compared IFN-γ production between the different groups of wild-type mice used in these experiments and found no significant difference (Extended Data 5, P=0.25 via one-way ANOVA). These data suggest that the amplification of memory CD4^{+} T cell responses seen the absence of *Nlrc4*^{-/-} is driven by NLRP3 activation, while NLRP3 does not have an effect when NLRC4 is active.

NLRC4 restricts NLRP3-dependent production of IL-18 and IFN-γ

In macrophages infected with *Salmonella* SL1344, NLRC4 is activated rapidly to induce caspase-1-mediated pyroptosis and IL-1β and IL-18 release[27], whilst NLRP3 activation is delayed to optimise IL-1β and IL-18 production without inducing pyroptosis[15,22]. Infection of wild-type and *Nlrp3*^{-/-} macrophages with *S.* Typhimurium M525P resulted in pyroptotic cell death within 2 hours of infection, while *Nlrc4*^{-/-} and *Nlrc4*^{-/-}*Nlrp3*^{-/-} cells lysed between 6 and 12 hours (Extended Data 6a). In the absence of NLRC4, cells produced IL-1β via NLRP3 and because these cells do not rapidly die, they secrete large amounts of IL-1β between 6 and 24 hours (Extended Data 6b).

Both IL-1β and IL-18 are involved in initiation and propagation of antigen-specific immunity against bacterial pathogens, therefore, we examined, whether NLRC4 and NLRP3 affect the production of these cytokines *in vivo* during infection with *S.* Typhimurium M525P. Serum IL-1β levels were below the detection limit, as expected[22], throughout the course of infection. In *Nlrc4^{-/-}* mice, levels of IL-18 were lower one day after challenge, but as the sublethal infection progressed, they markedly increased when compared to those detected in wild-type mice (Fig. 4b). This increase coincided with the onset of effector CD4^{+} T cell-driven microbial clearance with IL-18 remaining elevated in *Nlrc4^{-/-}* mice for a total of 3 weeks (Fig. 4b, day 7 to 28). This corresponds to the time that *Nlrc4^{-/-}* mice have heightened effector CD4^{+} T cell responses (Fig. 2a) suggesting a link between the increased levels of IL-18 and increased Th1 immunity.

We tested if this rise in serum IL-18 seen in *Nlrc4^{-/-}* mice was NLRP3-dependent. *Nlrp3^{-/-}* and *Nlrp3^{-/-}Nlrc4^{-/-}* mice, like *Nlrc4^{-/-}* mice, had decreased serum IL-18 levels very early during infection (Fig. 4b, Day 1), but, unlike *Nlrc4^{-/-}* mice, did not have increased IL-18 response as the infection progressed further (Fig. 4b, day 7-28). Importantly, *Nlrc4^{-/-}* and *Nlrp3^{-/-}Nlrc4^{-/-}* mice had similar bacterial burdens (Fig. 4a), but different IL-18 profiles (Fig. 4b), suggesting that this surge in serum IL-18 in the absence of NLRC4 depends on NLRP3 activation. IL-18 is a potent inducer of IFN-γ [28] which is indispensable for protection against *Salmonella*[20,29]. IFN-γ levels in *Nlrc4^{-/-}* mice remained elevated for 3 weeks compared to those in the *Nlrp3^{-/-}Nlrc4^{-/-}* mice (Fig. 4c, day 7 to 28) matching that of the serum IL-18 production. During the early stages of infection, cells such as natural killer cells are the main source of serum IFN-γ[30] explaining why at day 7 *Nlrc4^{-/-}* mice have higher levels of IFN-γ in the serum (Fig. 4c), but not when their CD4^{+} T cells are stimulated with bacterial extract *ex vivo* (Fig. 2a). Our data collectively suggest that, consistent with its role in downregulating CD4^{+} T cell memory responses, NLRC4 activation suppresses NLRP3-driven amplification of serum IL-18 and IFN-γ.

S. Typhimurium expressing flagellin from non-pathogenic *E. coli* evades NLRC4 recognition

Flagellin activates both TLR5 and NAIP/NLRC4 with the latter also recognising *Salmonella* type III secretory proteins such as PrgJ. TLR5 is important for generating T cell immunity against *S.* Typhimurium[31], but our data suggest that NLRC4 downregulates CD4^{+} T cell-mediated memory, while, at the same time, enhancing host survival during the early stages of a lethal infection (Extended Data 4a). We hypothesised that primary challenge with *Salmonella* genetically engineered to partially evade recognition by NLRC4, by mutating rather than deleting *fliC,* should retain TLR5 activation, enhance memory immunity and, therefore, potentially increase resistance to lethal re-challenge.

We genetically modified the wild-type M525P strain, which naturally lacks *fljB,* by replacing its native *fliC* with that from non-pathogenic *E. coli* K-12 substrain MG1655, to generate *S.* Typhimurium M525P fliC::fliC$_{MG1655}$ (M525P *fliC*$_{MG1655}$). Comparison of the predicted FliC proteins from *S.* Typhimurium and *E. coli* K-12 MG1655 showed high sequence homology at the N- and C-terminal regions of the protein, but with a variable central domain (Extended Data 7). Flagellin from this *E. coli* strain activates TLR5 as

efficiently as flagellin from S. Typhi but is impaired in activating NLRC4[32]. M525P *fliC*~MG1655~ also retains bacterial motility (Extended Data 8a) which may be important to facilitate infection and spread into the tissues. When tested *in vitro,* this mutant induced less cell death and IL-1β production than the wild-type strain in wild-type but not in *Nlrc4*^-/-^ macrophages, but could still activate NAIP1/2-NLRC4 signalling presumably via its type III secretion system (Extended Data 8b and 8c). TNF-α production by wild-type macrophages infected with M525P *fliC*~MG1655~ or M525P were comparable (Extended Data 8d) suggesting no deficit in TLR activation. These data indicate that M525P fliC~MG1655~ shows reduced, but not obliterated, NLRC4 inflammasome recognition.

Wild-type mice infected with M525P *fliC*~MG1655~ had a higher bacterial burden than those infected with M525P (Fig. 5a), comparable to that seen in *Nlrc4*^-/-^ mice challenged with M525P (Fig. 1a). Bacterial loads of M525P and M525P *fliC*~MG1655~ were similar in *Nlrc4*^-/-^ mice confirming that the increased spread of M525P *fliC*~MG1655~ into the tissues was NLRC4-dependent (Fig. 5b). Serum levels of IL-18 and IFN-γ were significantly increased for two weeks (Figures 5c and 5d, day 7 to 21) in mice infected with M525P *fliC*~MG1655~ when compared to mice infected with M525P, again comparable to the differences seen between wild-type and *Nlrc4*^-/-^ mice infected with M525P (compare Fig. 4b, 4c with Fig. 5c and 5d). Infection of wild type mice with M525P *fliC*~MG1655~ did not, however, induce as high levels, or as sustained production, of IL-18 as seen in *Nlrc4*^-/-^ mice infected with M525P (compare Fig. 4b with Fig. 5c). This is consistent with M525P *fliC*~MG1655~ retaining some residual capacity to activate NLRC4.

Primary challenge with *S.* Typhimurium M525P *fliC*~MG1655~ enhances CD4+ T cell memory responses and improves protection against lethal re-challenge

We compared the CD4+ T-cell memory responses between wild-type mice challenged with M525P or M525P *fliC*~MG1655~ and found them to be higher in the M525P *fliC*~MG1655~ group (Figure 6a), comparable to those seen in *Nlrc4*^-/-^ mice (Fig. 1c). To determine whether primary challenge with *S.* Typhimurium M525P *fliC*~MG1655~ would confer any resistance against lethal re-challenge, wild-type mice were systemically infected with M525P or M525P *fliC*~MG1655~ and allowed to clear the infection before re-challenge with fully virulent SL1344. Mice initially infected with M525P survived for 8.5 days while the survival rate of mice infected with M525P *fliC*~MG1655~ was markedly increased with approximately 75% of them surviving up to 21 days post-lethal re-challenge (Fig. 6b). Mice in the M525P *fliC*~MG1655~ group also lost less weight from day 4 to day 6 after re-challenge when compared to mice in the M525P group (Fig. 6c). These data suggest that reduced NLRC4 activation during primary challenge promotes protection against re-challenge although the mechanism by which this occurs is unclear.

Increased levels of serum IL-18 correlated with increased effector immunity (Fig. 2a and 4b), we, therefore, tested if IL-18 contributes to the amplification of CD4+ T cell immunity seen when NLRC4 activation is impaired. We compared the *ex vivo* memory responses between wild-type and *IL-18*^-/-^ *mice* challenged with M525P and found no difference suggesting that, when NLRC4 is fully activated, IL-18 does not affect the potency of the response (Fig. 6d). When mice were challenged with M525P *fliC*~MG1655~ however, the IFN-

γ response was reduced in *IL-18*^{-/-} mice and, although this did not quite meet statistical significance (Fig 6e, P=0.0513) is, nevertheless, suggestive of a link between NLRC4, IL-18 and CD4^{+} T cell-mediated Th1 memory.

Discussion

Pathogen-mediated activation of PRRs should determine the specificity of, and enhance the production of, antigen-specific immunity, yet here we show that activation of the PRR NLRC4 supresses memory CD4^{+} T cell-mediated responses against *Salmonella.* The CD4^{+} T cell-mediated immunity is critical for host control and long-term protection against intraphagosomal pathogens such as *Salmonella.* Equally important is the fact that mice initially challenged with a *Salmonella* strain that evades detection by NLRC4 were protected against an otherwise lethal rechallenge. This work, therefore, has important implications for vaccine development against pathogens that efficiently activate the NLRC4 inflammasome, such as *Legionella*[33]*, Pseudomonas*[34] and *Shigella* [35].

We used inflammasome-deficient mice to show that activation of NLRC4 by *S.* Typhimurium curtails antigen-specific CD4^{+} T cell-mediated memory responses and confirmed this phenotype by using a *Salmonella* mutant defective in activating NLRC4. In the wild-type strain we replaced native flagellin with flagellin from *E. coli* that is impaired in activating NLRC4, but can still activate TLR5 and keep the mutant motile, both of which could potentially affect the development of immunity against *Salmonella.* This mutant enhanced antigen-specific immunity, most likely by its clear ability to evade NLRC4 activation, but it would be interesting to test if a flagellin-deficient mutant would induce similar effects *in vivo*.

Relatively little is known about whether NLRC4 can affect the development of antigen-specific immunity against pathogens. Studies investigating the effect of NLRC4 on CD8+ T cell immunity have shown contrasting results. *Listeria monocytogenes* constitutively expressing flagellin from *Legionella pneumophila* suppressed CD8^{+} T cell immunity in mice and failed to protect them against re-challenge[36]. Flagellin recognition by NLRC4 during *Salmonella* infection, in contrast, induces IFN-γ release by memory CD8+ T cells[19]. A similar phenomenon has been described in Salmonella-induced CD4^{+} Th1 effector cells which require both NLRC4 and NLRP3 to optimally secrete IFN-γ in response to LPS and flagellin[18]. Unlike our work, however, both these studies describe a role for NLRC4 in non antigen-specific immune responses and suggest that NLRC4 activation drives the induction, rather than downregulation, of T cell responses.

Our data show that NLRC4 activation negatively regulates CD4^{+} T cell-mediated memory immunity against *Salmonella* via an NLRP3-dependent mechanism. *Salmonella* engages first NLRC4 and subsequently NLRP3 which maximises IL-1 p/IL-18 production *in vitro*[15,22] and is particularly important when NLRC4 activation is impaired. Our work shows that mice lacking NLRC4 have increased serum IL-18 levels only when they have functional NLRP3, while deficiency in both PRRs prevents IL-18 amplification in the serum. We hypothesise that during *S.* Typhimurium infection, NLRC4 prevents NLRP3 from amplifying cytokine production by APCs and this, in turn, restricts the potency of pathogen-

specific immune responses. Defective NLRC4 activation by increasing the levels of Th1-related cytokines in the serum enhances the expansion of antigen-specific CD4^{+} T cells and, consequently, this would give rise to a larger pool of memory cells. These cytokines could either be produced by the APCs during their interaction with naive T cells or by cells other than APCs at a later stage to act on activated effector T cells[4].

The NLRP3-dependent mechanism by which NLRC4 suppresses T cell memory responses is unclear but our data suggest that IL-18 could be important. IL-18 enhances Th1 antigen-specific immunity by increasing IFNg production from Th1 CD4^{+} T cells and natural killer cells[37]. It is also important for the maintenance of potent Th1 responses against *Listeria*[38] and promotes antigen-specific clonal expansion and survival of effector CD4^{+} T cells in response to flagellin[39]. In our model, elevated serum IL-18 coincides with increased CD4^{+} T cell effector responses and persists for two to three weeks during the microbial clearance phase when the vast majority of effector cells die and only a small fraction survive to become quiescent, long-lived memory cells[40]. We saw that when NLRC4 activation is defective, IL-18 deficiency partially prevents the amplification of memory responses. Other mechanisms may be important, however, such as the production of IL-1β which can enhance Th1 cell expansion[41] or cytokine-independent mechanisms, such as phagosome acidification, which can affect the development of adaptive immunity against Gram-positive bacteria[42].

In conclusion, here we describe an unknown mechanism by which reduced activation of a PRR, NLRC4, enhances antigen-specific memory responses and promotes long-term protection against re-challenge. This reveals a clear link between NLRC4 activation and restriction of pathogen-specific immunity within a physiological setting. Whether this phenomenon is induced by the pathogen as a strategy to impede the development of optimal memory responses or by the host to avoid immunopathology by tightly regulating levels of proinflammatory cytokines remains to be determined.

Methods

Mice

Wild-type C57BL/6J mice were obtained from Charles River, UK. *Nlrc4*^{-/-} and *Nlrp3*[--] mice on a C57BL/6J background (after at least 8 back crosses onto the C57BL/6J background) were kindly provided by Prof. Kate Fitzgerald (University of Massachusetts Medical School). The *Nlrc4*^{-/-}*Nlrp3*^{-/-} mice were generated in-house by crossing *Nlrc4*^{-/-} with *Nlrp3*^{-/-} mice. All mouse colonies were bred independently. Mice were genotyped by PCR using standard protocols. All mice were maintained in a specific pathogen-free facility according to the Animals Scientific Procedures outlined by the UK Home Office regulations. All work involving live animals complied with the University of Cambridge Ethics Committee regulations and was performed under the Home Office Project License numbers 80/2572 and P48B8DA35. Both male and female mice between 8 and 24 weeks of age were used in infection trials and as donors for primary bone marrow-derived macrophages (BMDMs).

Bacterial Strains and Animal Infections

S. Typhimurium strains SL1344 and M525P[43], strains of high and intermediate virulence, respectively, were used in this study. For *in vitro* studies, S. Typhimurium was grown from single colonies to exponential phase, by inoculating a 17.5h overnight culture 1 in 10 into LB broth and incubating at 37°C, 200 rpm for 2h. For *in vivo* infections, stationary phase S. Typhimurium cultures were washed and resuspended in Dulbecco's PBS (D-PBS, Sigma). For i.v. challenge experiments, 0.2ml of the inoculum were administered systemically via the lateral tail vein. For oral challenge experiments, mice were lightly anesthetized with isoflurane and then inoculated with 0.2 mL of the inoculum via oral gavage. Control mice were inoculated with sterile PBS only. The exact dose of *Salmonella* administered was determined by serial dilution and plating the inoculum on LB plates before and after infection. Primary challenge in all experiments was performed by i.v. administration of approximately 10^4 CFU S. Typhimurium 525P wild-type or mutant per mouse unless mentioned otherwise. Exact doses for each experiment are given in the legends of the respective graphs. All experiments were performed after approval from the University of Cambridge ethical review committee and under the UK government Home office regulations license numbers 80/2135, 80/11763, PF86EABB1 and P48B8DA35. In this work, no statistical methods were used to predetermine the sample size. The experiments were not randomized, and the investigators were not blinded to allocation during the experiments and outcome assessments.

Humane endpoint curves

In animal trials which involved re-challenge with fully virulent S. Typhimurium, we constructed humane endpoint curves as an alternative to survival curves. To do this, mice were weighed once and assessed twice daily for manifestation of clinical signs associated with generalized infection. These include weight loss of over 15% of maximum body weight, marked piloerection, subdued behavioural pattern even when provoked and reduced exploration, isolation from peers, intermittent hunched posture and persistent oculo-nasal discharge. Mice would be euthanized without delay when any of these signs persisted for more than 12 hours.

Bacterial Isolation and Enumeration

Mice were euthanized at specific intervals following infection and their spleens and livers removed aseptically. Organs were homogenized in 10ml sterile water using a Colworth stomacher. Organ homogenates were serially diluted and plated on LB agar plates. LB plates were incubated overnight at 37 °C followed by enumeration of colony-forming units. In some experiments, spleens were first passed through a cell strainer to produce single cell suspensions in RPMI, a fraction of which was then used for bacterial enumeration.

Construction of S. Typhimurium M525P *fliC::fliC* $_{E.coli}$ and bacterial motility assays

To engineer S. Typhimurium that expresses the FliC protein of the non-pathogenic E. *coli* K-12 strain MG1655, a DNA fragment was synthesized by GeneArt Gene Synthesis (Life Technologies) encoding E. *coli* K-12 MG1655 *fliC* adjacent to a chloramphenicol resistance cassette (Cm^R) and flanked by 60 bp arms homologous to the sequence immediately

upstream and downstream of *S.* Typhimurium M525P *fliC.* This *fliC*$_{MG1655}$ cassette was transformed into electrocompetent *S.* Typhimurium M525P cells carrying the pBADλRed plasmid[44,45]. Transformants were selected on LB agar supplemented with 25 ug/ml chloramphenicol and positive clones were confirmed by sequencing. The growth rate of the mutant strain was assessed by performing viable bacterial counts and found to be similar to that of the wild-type strain (Supplementary Fig. 1).

To assess bacterial motility, overnight cultures grown in LB broth were diluted into fresh LB broth to an OD600 of 0.05 and grown at 37°C until cultures reached an OD600 of 1.0. Two microliters of culture were inoculated into 0.25% tryptone agar (2.5g/l agar, 10g/L tryptone, 5g/L NaCl). Plates were incubated at 37°C for between 4 and 6 hours and swarm diameter was measured.

Cell Culture and Infections

BMDMs were prepared as previously described[46]. They were infected with *S.* Typhimurium grown to exponential phase as previously described[47]. Cell viability was assessed using the Cytotox 96 Non-Radioactive Cytotoxicity assay (Promega).

CD4$^+$ T Cell *Ex Vivo* Stimulation Assays

Mice were euthanized, their spleens aseptically removed and, after mechanical disruption, passed through a 70 μm cell strainer (BD Biosciences) to obtain single cell suspensions in pre-warmed RPMI containing 2% (vol/vol) FCS (Hyclone). Cell suspensions were washed once and resuspended in Red Blood Cell Lysis buffer (Sigma), mixed and incubated for 10 min on ice. Total splenocytes were washed twice and passed through a 30μ m filter (Partec). CD4$^+$ T cells were purified using CD4 microbeads and magnetic positive selection according to manufacturer's guidelines (Miltenyi Biotec). This routinely resulted in cell populations containing over 95% CD4$^+$ cells. CD4$^+$ T cells were resuspended in complete RPMI medium containing 10% FCS (Hyclone), 5mM L-glutamine, 100U/ml penicillin, 100μg/ml streptomycin, 1mM HEPES and 0.02mM b-mercaptoethanol. Cells were seeded at 2 x 10^5 cells/well in round bottom 96-well plates (Greiner Bio-One) together with wild-type naïve total splenocytes previously treated (1h at 37°C and 5% CO2) with Mitomycin C 25 μg/ml (Sigma) at a 1:1 ratio (total cell number of 4 x 10^5 cells/well). Co-cultures from each mouse were either left unstimulated, stimulated with 2 μg/mL anti-mouse CD3e (clone 145-2C11, ebioscience) or 20 μg/mL whole *Salmonella* cell extract, prepared as described previously[48] and incubated at 37°C and 5% CO2. In some experiments, the polyclonal stimulus was provided by concanavalin A (rather than anti-mouse CD3e) which was used at a final concentration of 5 μg/mL. Cell culture supernatants were collected after 24h and 72h incubation for cytokine quantification. When CD4$^+$ T Cells were stimulated *ex vivo* to assess memory immunity, it was important to confirm that the primary infection has cleared and the effector immune response subsided. For this reason, any mice whose microbial load was above detection limit (20 CFU for the spleen and 10 CFU for the liver) were not included in the study.

ELISPOT and Cytokine Secretion Assay

The numbers of CD4^{+} T cells secreting IFN-γ were assessed by ELISPOT and cytokine secretion assays. For ELISPOT, capture and detection antibodies supplied by the mouse IFN-γ ELISpot Development Module (R&D Systems) were used according to manufacturer's guidelines. Briefly, co-cultures of purified CD4^{+} T cells with syngeneic feeder cells were incubated in duplicate wells in the presence or absence of whole *Salmonella* cell extract for 12 hours. Cell suspensions were then transferred in two-fold serial dilutions to a capture antibody-coated 96 well filtration plate (Millipore) and incubated for a further 12 hours. ELISpot Blue Colour Module (R&D Systems) analysis of the cell supernatant was performed according to manufacturer's guidelines. Data were expressed as IFN-γ spot-forming cells per 10^6 cells. The number of CD4^{+} T cells secreting IFN-γ was also determined using a flow cytometry-based cytokine secretion assay (Miltenyi Biotec) according to manufacturer's guidelines. To reduce non-specific background staining and increase sensitivity, cells were simultaneously stained with a fixable viability dye and anti-mouse CD4 antibody (clone GK1.5) (both from Invitrogen) while the sequential gating strategy used is shown in Supplementary Fig. 2. Data from 100,000 viable cells were acquired from each mouse using a DxP Multi-color updated FACSCan (BD) analysed with FlowJo Software (TreeStar). In subsequent experiments, cells were also stained with anti-mouse CD44 (clone IM7) and CD62L (clone MEL-14) during cytokine secretion assay to better characterise the class of memory CD4^{+} T cells secreting IFN-γ (effector or central memory). The sequential gating strategy for these analyses is shown in Extended Data 3. In this case, data from 100,000 viable cells were acquired from each mouse using an Attune NxT Flow Cytometer (Invitrogen) and analysed with FlowJo Software (TreeStar).

ELISA and Multiplex Immunoassays for Cytokine Quantification

Cytokine levels were measured in the serum and cell culture supernatant by bead-based, multiple cytokine detection immunoassay and/or ELISA analysis. Mouse serum was analysed via ELISA for levels of IL-1β (BD OptEIA set) and IL-18 (MBL International) and via multiplex immunoassays (ProcartaPlex, Invitrogen) for IFN-γ and TNF-α. Cell culture supernatant harvested from the CD4^{+} T cell stimulation assays was analysed by ELISA for levels of IFN-γ and IL-2 (DuoSet Development kit, R&D Systems) and a flow cytometric, bead based immunoassay (FlowCytomix, ebioscience) for simultaneous detection of mouse GM-CSF, IL-6, and TNF-α. IL-1β production from BMDMs infected with *Salmonella* was also analysed by ELISA. ELISAs and multiplex immunoassays were performed according to manufacturer's guidelines.

Detection of Serum Anti-LPS Antibodies

Antibody (Ab) titers against *S.* Typhimurium LPS were measured in the serum of infected and control mice by ELISA as previously described [49]. Serum Ab titers were calculated based on a standard curve constructed by 2-fold serial dilutions of the same positive serum sample run on every plate. The dilution at which OD450-OD570 of the standard sample approximated the value of 1 was arbitrarily appointed as 1000 Units.

Statistical Analyses

All statistical analyses were performed with GraphPad Prism version 8 with each specific analysis described in the appropriate figure legend. Exact p values are shown on each graph separately with $p < 0.05$ considered statistically significant.
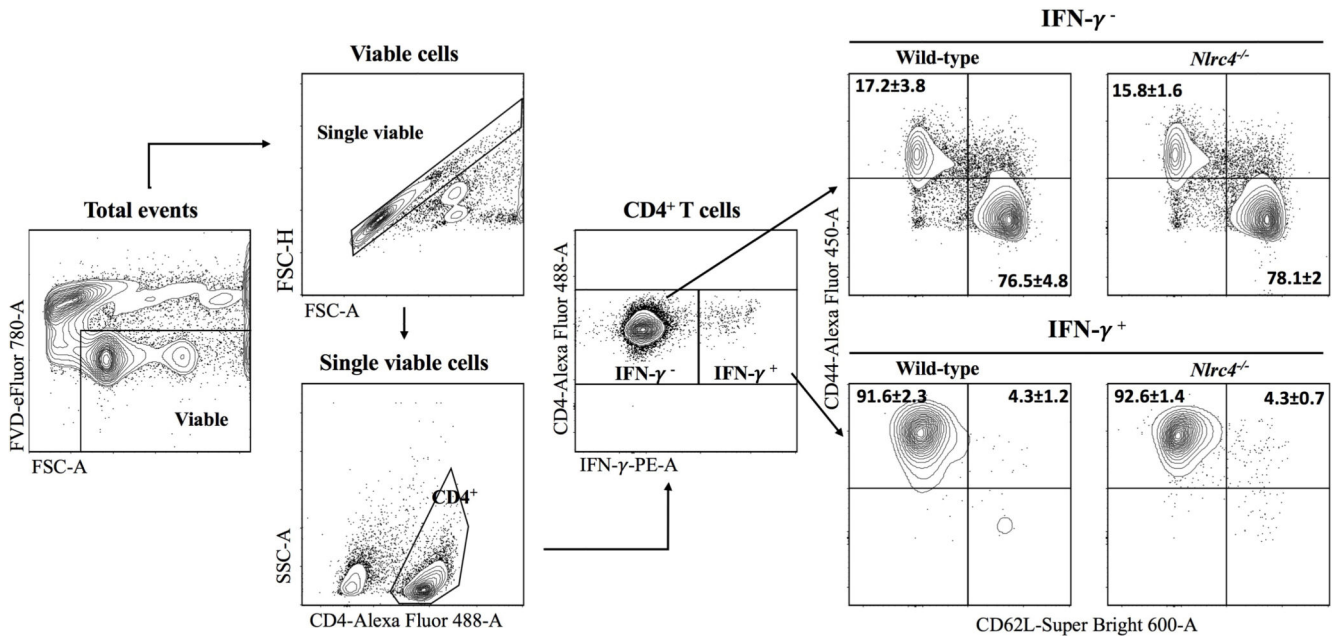
Extended Data
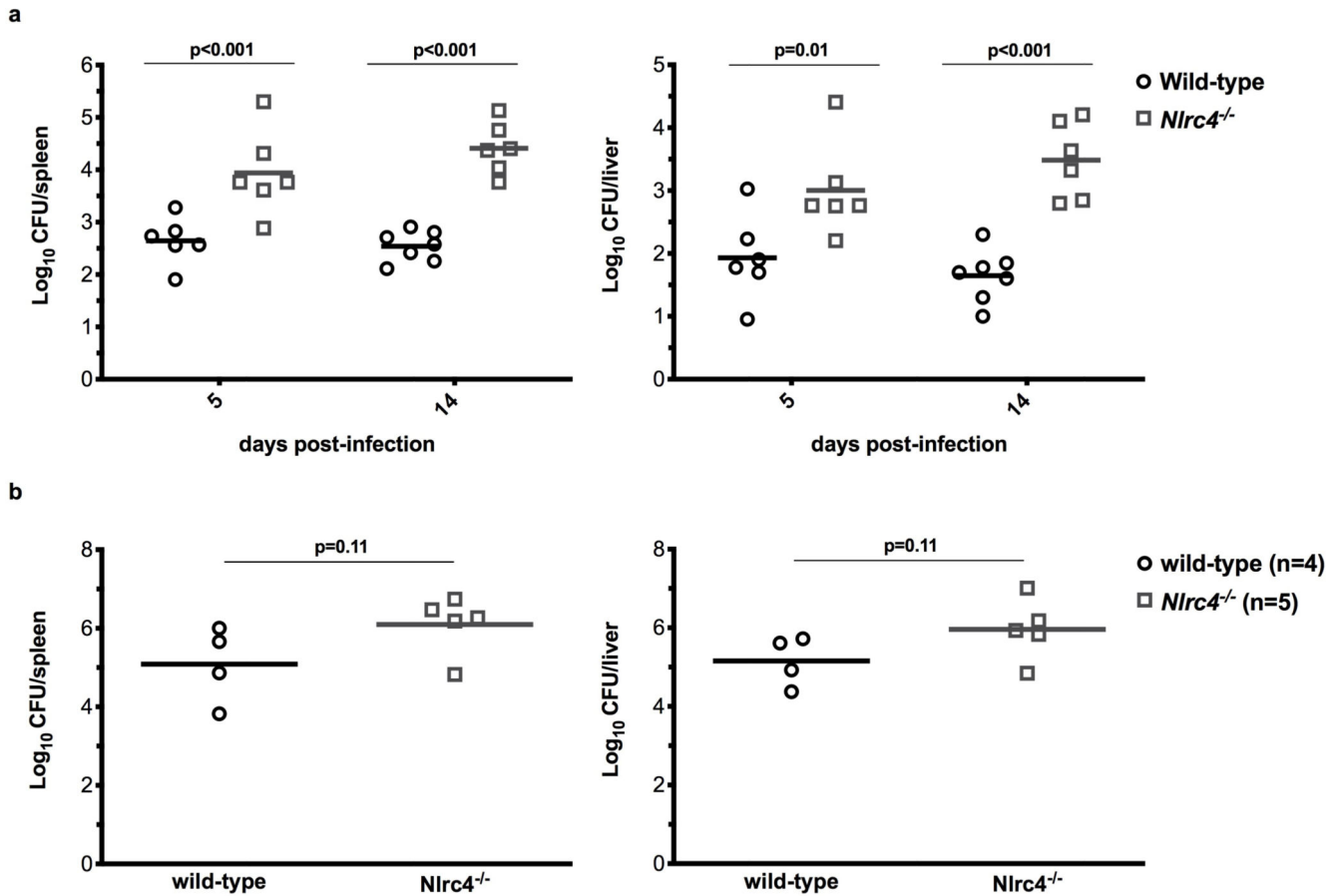
Extended Data Figure 1. NLRC4 is required to restrict microbial spread during an oral sub-lethal but not an oral lethal infection with *S*. Typhimurium

a, Wild type and *nlrc4*^{-/-} mice were challenged orally with 4.4×10^9 CFU *S*. Typhimurium M525P to establish a sub-lethal infection and microbial burden was determined in the spleen and liver at 5 days (n=6 for wild-type and *nlrc4*^{-/-}) and 14 days (n=7 for wild-type and n=6 for *nlrc4*^{-/-}) post-challenge. **b,** Wild type and *nlrc4*^{-/-} mice were challenged orally 8×10^8 CFU *S*. Typhimurium SL1344 to establish a lethal infection and microbial burden was determined in the spleen and liver at 4 days postchallenge. Each symbol represents one mouse and horizontal lines delineate the mean. Statistical significance was calculated by 2-way ANOVA followed by Sidak's multiple comparisons test for **a** and two-tailed Mann Whitney test for **b**. Data are representative of two independent experiments.
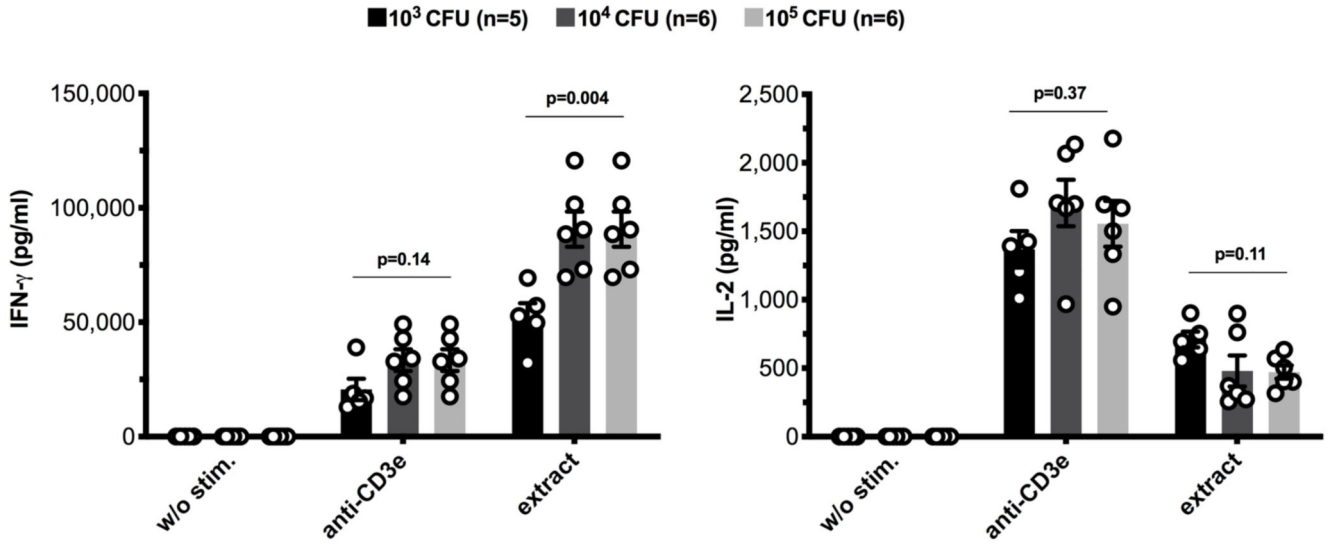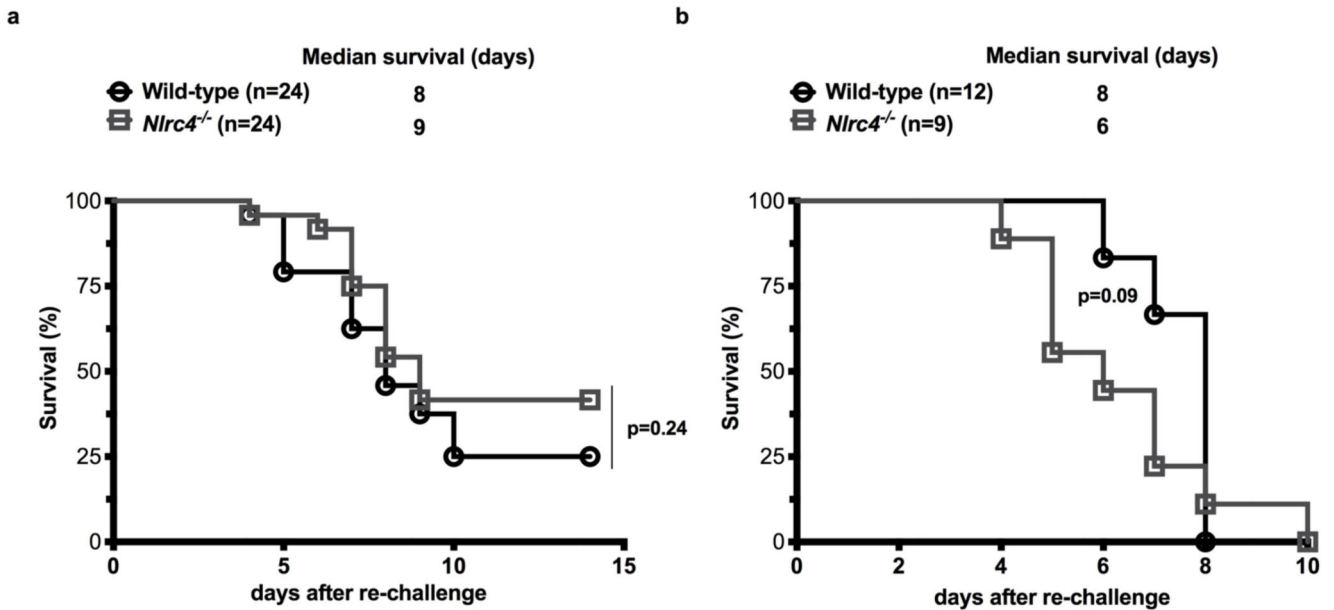
Extended Data Figure 2. The effect of infection dose on the potency of *ex vivo* CD4+ T cell-mediated responses.

Wild-type mice were challenged with either 1.58×10^5 CFU, 1.72×10^4 CFU or 1.53×10^3 CFU *S.* Typhimurium M525P. Mice were euthanised 104-125 days after challenge and their splenic CD4+ T cells were stimulated with medium only (w/o stim.), anti-mouse CD3e (anti-CD3e) or whole bacterial cell extract (extract). **a,** IFN-γ measured by ELISA in the cell culture supernatant after 72 hours. **b,** IL-2 measured by ELISA in the cell culture supernatant after 24 hours. Data are shown as mean ± SEM. Statistical significance was calculated by a one-way ANOVA. Data were generated from one experiment.


Extended Data Figure 3. Flow cytometric analysis reveals that CD4+ T cells secreting IFN-γ *ex vivo* have the profile of effector memory, rather than central memory, CD4+ T cells.

CD4^{+} T cells isolated from the spleen of wild-type and *nlrc4*^{-/-} mice 100 days after primary challenge with 1.24×10^4 CFU *S*. Typhimurium M525P were stimulated *ex vivo* with whole bacterial cell extract and phenotypically characterised via flow cytometry. Viable cells were first selected using a fixable viability dye (FVD) and single cells only were further included in the analysis based on their forward scatter area *vs.* forward scatter height. Single viable cells expressing CD4 were then separated to IFN-γ- and IFN-γ+ with both groups analysed for expression of CD44 and CD62L. For CD4^{+}IFN-γ cells, the phenotype CD44+CD62- represents effector T cells, while the phenotype CD44-CD62+ represents naïve T cells. For CD4^{+}IFN-γ+ cells, the phenotype CD44^{+}CD62- represents effector memory T cells, while the phenotype CD44+CD62+ represents central memory T cells. Percentages shown in the respective quadrants are mean values ± SD from N=5 wild-type and N=6 *Nlrc4*^{-/-} mice. Data were generated from one experiment.


Extended Data Figure 4. NLRC4 does not affect protection against lethal rechallenge
Wild-type and *nlrc4*^{-/-} mice were challenged with either sterile PBS (naïve) or $1-1.15 \times 10^4$ CFU *S*. Typhimurium M525P and allowed to clear the primary infection for 90-106 days. They were then re-challenged orally with $1.37-7.2 \times 10^7$ CFU *S*. Typhimurium SL1344 to establish a lethal infection and inspected twice daily. They were euthanized upon detection of adverse signs and a humane end point curve was constructed for **a,** naïve mice and **b,** mice "immunised" with *Salmonella.* Data has been pooled from 2 independent experiments. Statistical significance was calculated by a two-sided log-rank test.
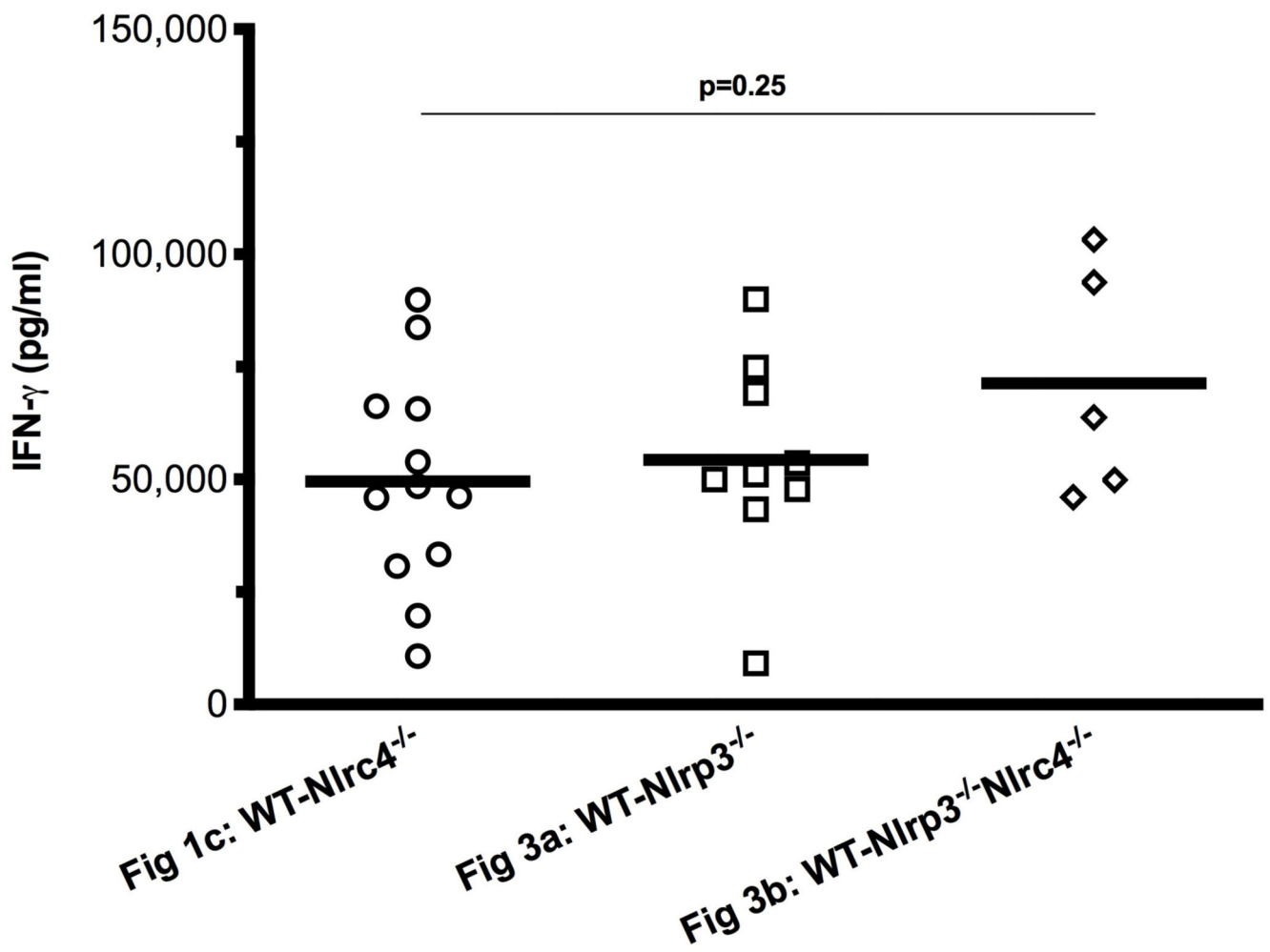
Extended Data Figure 5. Data variation between independent trials comparing CD4+ T cell-mediated responses in wild-type, *nlrc4*-/-, *nlrp3*-/- and *nlrp3*-/-*nlrc4*-/- mice is not statistically significant.

Levels of IFN-γ produced by CD4+ T cells stimulated *ex vivo* with whole bacterial cell extract were compared between wild-type mice used in three independent trials shown in Figure 1c, Figure 3 a and Figure 3b. Each symbol represents one mouse and horizontal lines delineate the mean. The data was tested for statistical significance by one-way ANOVA.
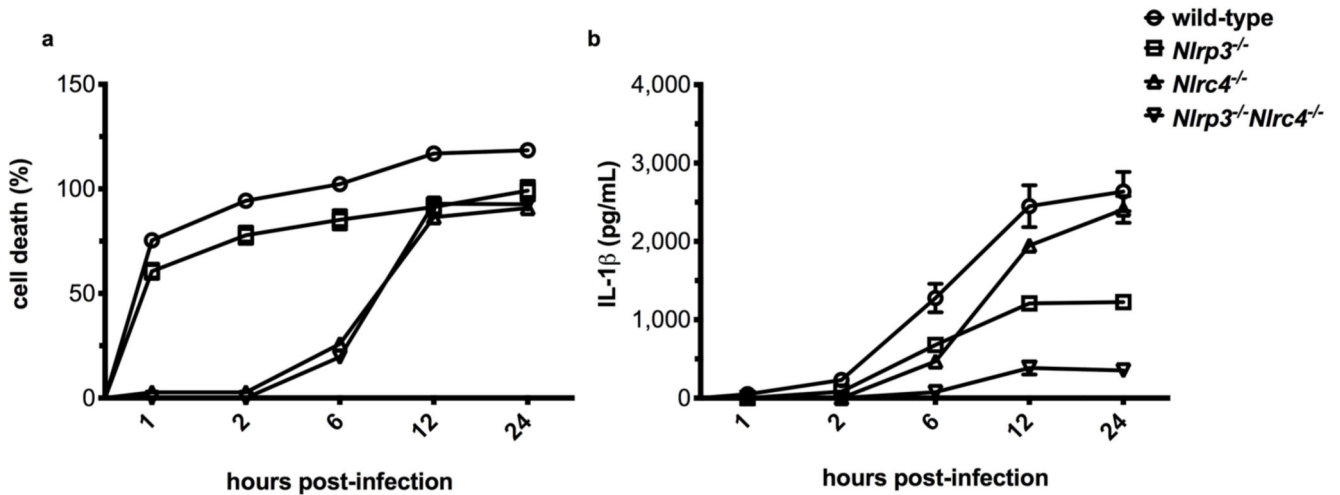
Extended Data Figure 6. In the absence of NLRC4, Salmonella-infected macrophages do not undergo early cell death enabling them to survive longer and secrete IL-1β via activation of NLRP3.

Unprimed bone marrow derived macrophages (BMDMs) from wild-type, *nlrc4*^{-/-}, *nlrp3*^{-/-} and *nlrc4*^{-/-}*nlrp3*^{-/-} mice were infected with *S*. Typhimurium M525P in logarithmic growth at the MOI=50. **a,** Cytotoxicity was determined by measuring levels of LDH released in the cell culture supernatant. **b**, Levels of IL-1β were determined by ELISA in the cell culture supernatant. Data are shown as mean of triplicate wells ± SEM. Data are representative of two independent experiments.

```
M525P    MAQVINTNSLSLLTQNNLNKSQSALGTAIERLSSGLRINSAKDDAAGQAIANRFTANIKG    60
MG1655   MAQVINTNSLSLITQNNINKNQSALSSSIERLSSGLRINSAKDDAAGQAIANRFTSNIKG    60
         ***********:****:**.****.::***************************:****


M525P    LTQASRNANDGISIAQTTEGALNEINNNLQRVRELAVQSANSTNSQSDLDSIQAEITQRL    120
MG1655   LTQAARNANDGISVAQTTEGALSEINNNLQRVRELTVQATTGTNSESDLSSIQDEIKSRL    120
         ****:********:*******.************:**::..***:***.*** **..**


M525P    NEIDRVSGQTQFNGVKVLAQDNTLTIQVGANDGETIDIDLKQINSQTLGLDTLNVQQKYK    180
MG1655   DEIDRVSGQTQFNGVNVLAKNGSMKIQVGANDNQTITIDLKQIDAKTLGLDGFSVKNNDT    180
         :**************:***::..::.*******.:** ******:::***** :.*::.


M525P    VSDTAATVTGYADTT---IALDNSTFKA-SATGLGGTDQKIDGDLKFDDTTGKYYAKVTV    236
MG1655   VTTSA-PVTAFGATTTTNNIKLTGITLSTEAATDTGGTNPA-SIEGVYTDNGNDYYAKI--    236
         *: :* **.:. **    * * . *:.: :**. ***:    .: : *. ..****:


M525P    TGGTGKDGYYEVSVDKTNGEVTLAGGATSPLTGGLPATATEDVKNVQVANADLTEAKAAL    296
MG1655   TGGDNDGKYYAVTVAN-DGTVTMATGATANATVTDANT--TKATTITSGGTPVQIDNTAG    293
         ***  ... ** *:* : :* **:* ***:   *      *    ...: ..: :   ::*


M525P    TAAGVTGTASVVKMSYTDNNGKTIDG-GLAVKVGDDYYSATQNKDGSISINTTKYTADDG    355
MG1655   SATANLGAVSLVKLQ--DSKGNDTDTYALKDTNGNLYAADVNETTGAVSVKTITYTDSSG    351
         :*:.  *:.*:**:.  *.:*: * .* . *: * : .::. *::*::* .** ..*


M525P    T-SKTALNKLGGADGKTEVVSIGGKTYAASKAEGHNFKAQPD-----LAEAAATTTENPL    409
MG1655   AASSPTAVKLGGDDGKTEVVDIDGKTYDSADLNGGNLQTGLTAGGEALTAVANGKTTDPL    411
         : *. :  **** *******.*.**** ::. :* *:::       *: .*  .* :**


M525P    QKIDAALAQVDTLRSDLGAVQNRFNSAITNLGNTVNNLTSARSRIEDSDYATEVSNMSRA    469
MG1655   KALDDAIASVDKFRSSLGAVQNRLDSAVTNLNNTTTNLSEAQSRIQDADYATEVSNMSKA    471
         : :* *:*.**.:**.*******:.**:***.**..**:.*:***:*:**********:*


M525P    QILQQAGTSVLAQANQVPQNVLSLLR-    495
MG1655   QIIQQAGNSVLAKANQVPQQVLSLLQG    498
         **:****.****:******:*****:
```

Extended Data Figure 7. Pairwise Sequence Alignment of FliC from *E. coli* K-12 MG1655 and *S.* Typhimurium M525P.

Comparison of the predicted FliC proteins from *S.* Typhimurium M525P and *E. coli* K-12 MG1655 by Clustal Omega (EMBL-EBI).
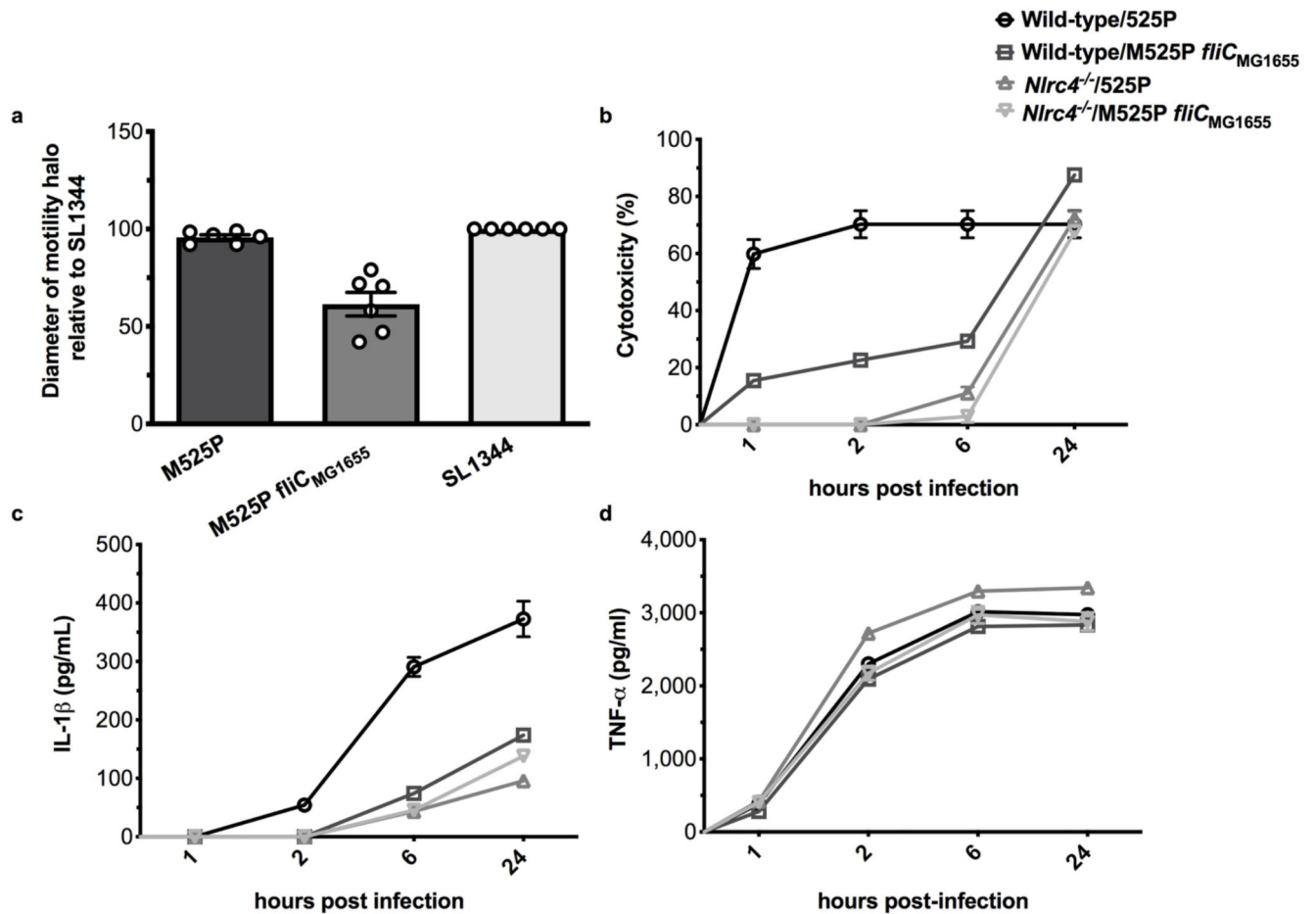
Extended Data Figure 8. *Salmonella* **expressing flagellin from non-pathogenic *E. coli* (M525P *fliC* MG1655) is motile but impaired at activating the NLRC4 inflammasome in macrophages.** Comparison of the motility diameter between *S.* Typhimurium M525P, M525P *fliC* MG1655 and SL1344. Data are expressed as % of the diameter achieved by the SL1344. **b-d**, Unprimed bone marrow derived macrophages from wild-type and *nlrc4⁻/⁻* mice were infected for lh, 2h, 6h and 24h with *S.* Typhimurium M525P or M525P fliC MG1655 in logarithmic growth. **b**, Cytotoxicity was determined by measuring levels of LDH released in the cell culture supernatant at an MOI of 50. **c**, Levels of IL-lβ and **d,** TNF-α were determined by ELISA in the cell culture supernatant at an MOI of 1. Data has been pooled from 6 independent experiments and shown as mean ± SEM in **a**. Data are representative of two independent experiments in **b-d** and shown as mean of triplicate wells ± SEM.

Acknowledgments

Data Availability

All data used to generate the figures presented in this work are available in Cambridge Research Repository Apollo with the identifier https://doi.org/10.17863/CAM.41575

References

1. Takeda K, Akira S. Toll-like receptors. Current protocols in immunology. 2015; 109

2. Gross O, Thomas CJ, Guarda G, Tschopp J. The inflammasome: an integrated view. Immunol Rev. 2011; 243:136–151. [PubMed: 21884173]

3. Iwasaki A, Medzhitov R. Control of adaptive immunity by the innate immune system. Nat Immunol. 2015; 16:343–353. [PubMed: 25789684]

4. Evavold CL, Kagan JC. How Inflammasomes Inform Adaptive Immunity. J Mol Biol. 2018; 430:217–237. [PubMed: 28987733]

5. McSorley SJ, Cookson BT, Jenkins MK. Characterization of CD4+ T cell responses during natural infection with Salmonella typhimurium. J Immunol. 2000; 164:986–993. [PubMed: 10623848]

6. Miao EA, et al. Cytoplasmic flagellin activates caspase-1 and secretion of interleukin 1 beta via Ipaf. Nat Immunol. 2006; 7:569–575. [PubMed: 16648853]

7. Franchi L, et al. Cytosolic flagellin requires Ipaf for activation of caspase-1 and interleukin 1 beta in salmonella-infected macrophages. Nat Immunol. 2006; 7:576–582. [PubMed: 16648852]

8. Miao EA, et al. Innate immune detection of the type III secretion apparatus through the NLRC4 inflammasome. P Natl Acad Sci USA. 2010; 107:3076–3080.

9. Lightfield KL, et al. Critical function for Naip5 in inflammasome activation by a conserved carboxy-terminal domain of flagellin. Nat Immunol. 2008; 9:1171–1178. [PubMed: 18724372]

10. Zhao Y, et al. The NLRC4 inflammasome receptors for bacterial flagellin and type III secretion apparatus. Nature. 2011; 477:596–U257. [PubMed: 21918512]

11. Kofoed EM, Vance RE. Innate immune recognition of bacterial ligands by NAIPs determines inflammasome specificity. Nature. 2011; 477:592. [PubMed: 21874021]

12. Martinon F, Burns K, Tschopp J. The inflammasome: A molecular platform triggering activation of inflammatory caspases and processing of proIL-beta. Mol Cell. 2002; 10:417–426. [PubMed: 12191486]

13. Broz P, Dixit VM. Inflammasomes: mechanism of assembly, regulation and signalling. Nat Rev Immunol. 2016; 16:407–420. [PubMed: 27291964]

14. Ding J, Shao F. Growing a gasdermin pore in membranes of pyroptotic cells. The EMBO journal. 2018; 37

15. Man SM, et al. Inflammasome activation causes dual recruitment of NLRC4 and NLRP3 to the same macromolecular complex. Proc Natl Acad Sci U S A. 2014; 111:7403–7408. [PubMed: 24803432]

16. Qu Y, et al. NLRP3 recruitment by NLRC4 during Salmonella infection. J Exp Med. 2016; 213:877–885. [PubMed: 27139490]

17. Garlanda C, Dinarello CA, Mantovani A. The interleukin-1 family: back to the future. Immunity. 2013; 39:1003–1018. [PubMed: 24332029]

18. O'donnell H, et al. Toll-like Receptor and Inflammasome Signals Converge to Amplify the Innate Bactericidal Capacity of T Helper 1 Cells. Immunity. 2014; 40:213–224. [PubMed: 24508233]

19. Kupz A, et al. NLRC4 inflammasomes in dendritic cells regulate noncognate effector function by memory CD8(+) T cells. Nat Immunol. 2012; 13:162–169. [PubMed: 22231517]

20. Hess J, Ladel C, Miko D, Kaufmann SHE. Salmonella typhimurium aroA(-) infection in gene-targeted immunodeficient mice - Major role of CD4(+) TCR-alpha beta cells and IFN-gamma in bacterial clearance independent of intracellular location. J Immunol. 1996; 156:3321–3326. [PubMed: 8617956]

21. Nauciel C. Role of Cd4+ T-Cells and T-Independent Mechanisms in Acquired-Resistance to Salmonella-Typhimurium Infection. J Immunol. 1990; 145:1265–1269. [PubMed: 1974274]

22. Broz P, et al. Redundant roles for inflammasome receptors NLRP3 and NLRC4 in host defense against Salmonella. J Exp Med. 2010; 207:1745–1755. [PubMed: 20603313]

23. Lara-Tejero M, et al. Role of the caspase-1 inflammasome in Salmonella typhimurium pathogenesis. J Exp Med. 2006; 203:1407–1412. [PubMed: 16717117]

24. Mastroeni P, Simmons C, Fowler R, Hormaeche CE, Dougan G. Igh-6(-/-) (B-cell-deficient) mice fail to mount solid acquired resistance to oral challenge with virulent Salmonella enterica serovar typhimurium and show impaired Th1 T-cell responses to Salmonella antigens. Infect Immun. 2000; 68:46–53. [PubMed: 10603367]

25. Heng TSP, Painter MW, Project IG. The Immunological Genome Project: networks of gene expression in immune cells. Nat Immunol. 2008; 9:1091–1094. [PubMed: 18800157]

26. Bruchard M, et al. The receptor NLRP3 is a transcriptional regulator of TH2 differentiation. Nat Immunol. 2015; 16:859–870. [PubMed: 26098997]

27. Mariathasan S, et al. Differential activation of the inflammasome by caspase-1 adaptors ASC and Ipaf. Nature. 2004; 430:213–218. [PubMed: 15190255]

28. Tsutsui H, Matsui K, Okamura H, Nakanishi K. Pathophysiological roles of interleukin-18 in inflammatory liver diseases. Immunol Rev. 2000; 174:192–209. [PubMed: 10807517]

29. Mastroeni P, Villarrealramos B, Hormaeche CE. Role of T-Cells, Tnf-Alpha and Ifn-Gamma in Recall of Immunity to Oral Challenge with Virulent Salmonellae in Mice Vaccinated with Live Attenuated Aro-Salmonella Vaccines. Microb Pathogenesis. 1992; 13:477–491.

30. Kupz A, et al. Contribution of Thy1(+) NK cells to protective IFN-gamma production during Salmonella Typhimurium infections. P Natl Acad Sci USA. 2013; 110:2252–2257.

31. Letran SE, et al. TLR5-Deficient Mice Lack Basal Inflammatory and Metabolic Defects but Exhibit Impaired CD4 T Cell Responses to a Flagellated Pathogen. J Immunol. 2011; 186:5406–5412. [PubMed: 21451112]

32. Yang J, et al. Flagellins of Salmonella Typhi and nonpathogenic Escherichia coli are differentially recognized through the NLRC4 pathway in macrophages. J Innate Immun. 2014; 6:47–57. [PubMed: 23816851]

33. Amer A, et al. Regulation of Legionella phagosome maturation and infection through flagellin and host Ipaf. J Biol Chem. 2006; 281:35217–35223. [PubMed: 16984919]

34. Franchi L, et al. Critical role for Ipaf in Pseudomonas aeruginosa-induced caspase-1 activation. Eur J Immunol. 2007; 37:3030–3039. [PubMed: 17935074]

35. Suzuki T, et al. Differential regulation of caspase-1 activation, pyroptosis, and autophagy via Ipaf and ASC in Shigella-infected macrophages. Plos Pathog. 2007; 3:e111. [PubMed: 17696608]

36. Sauer JD, et al. Listeria monocytogenes engineered to activate the Nlrc4 inflammasome are severely attenuated and are poor inducers of protective immunity. P Natl Acad Sci USA. 2011; 108:12419–12424.

37. Yoshimoto T, et al. IL-12 up-regulates IL-18 receptor expression on T cells, Th1 cells, and B cells: Synergism with IL-18 for IFN-gamma production. J Immunol. 1998; 161:3400–3407. [PubMed: 9759857]

38. Neighbors M, et al. A critical role for interleukin 18 in primary and memory effector responses to Listeria monocytogenes that extends beyond its effects on Interferon gamma production. J Exp Med. 2001; 194:343–354. [PubMed: 11489953]

39. Maxwell JR, et al. IL-18 bridges innate and adaptive immunity through IFN-gamma and the CD134 pathway. J Immunol. 2006; 177:234–245. [PubMed: 16785519]

40. Pepper M, Jenkins MK. Origins of CD4(+) effector and central memory T cells. Nat Immunol. 2011; 12:467–471. [PubMed: 21739668]

41. Ben-Sasson SZ, et al. IL-1 acts directly on CD4 T cells to enhance their antigen-driven expansion and differentiation. P Natl Acad Sci USA. 2009; 106:7119–7124.

42. Sokolovska A, et al. Activation of caspase-1 by the NLRP3 inflammasome regulates the NADPH oxidase NOX2 to control phagosome function. Nat Immunol. 2013; 14:543–+. [PubMed: 23644505]

43. Mastroeni P, et al. Antimicrobial actions of the NADPH phagocyte oxidase and inducible nitric oxide synthase in experimental salmonellosis. II. Effects on microbial proliferation and host survival in vivo. J Exp Med. 2000; 192:237–247. [PubMed: 10899910]

44. Datsenko KA, Wanner BL. One-step inactivation of chromosomal genes in Escherichia coli K-12 using PCR products. Proc Natl Acad Sci U S A. 2000; 97:6640–6645. [PubMed: 10829079]

45. Mo E, Peters SE, Willers C, Maskell DJ, Charles IG. Single, double and triple mutants of Salmonella enterica serovar Typhimurium degP (htrA), degQ (hhoA) and degS (hhoB) have diverse phenotypes on exposure to elevated temperature and their growth in vivo is attenuated to different extents. Microb Pathog. 2006; 41:174–182. [PubMed: 16949246]

46. Man SM, et al. Inflammasome activation causes dual recruitment of NLRC4 and NLRP3 to the same macromolecular complex. P Natl Acad Sci USA. 2014; 111:7403–7408.

47. Man SM, et al. Salmonella Infection Induces Recruitment of Caspase-8 to the Inflammasome To Modulate IL-1 beta Production. J Immunol. 2013; 191:5239–5246. [PubMed: 24123685]

48. Harrison JA, VillarrealRamos B, Mastroeni P, DeHormaeche RD, Hormaeche CE. Correlates of protection induced by live Aro(-) Salmonella typhimurium vaccines in the murine typhoid model. Immunology. 1997; 90:618–625. [PubMed: 9176117]

49. Dehormaeche RD, Jessop H, Bundell C. Antibodies to the C-Epitope of Neisseria-Gonorrhoeae Are Present in Patients with Gonorrhea and Absent in Normal Sera. J Gen Microbiol. 1988; 134:1289–1297. [PubMed: 2462011]
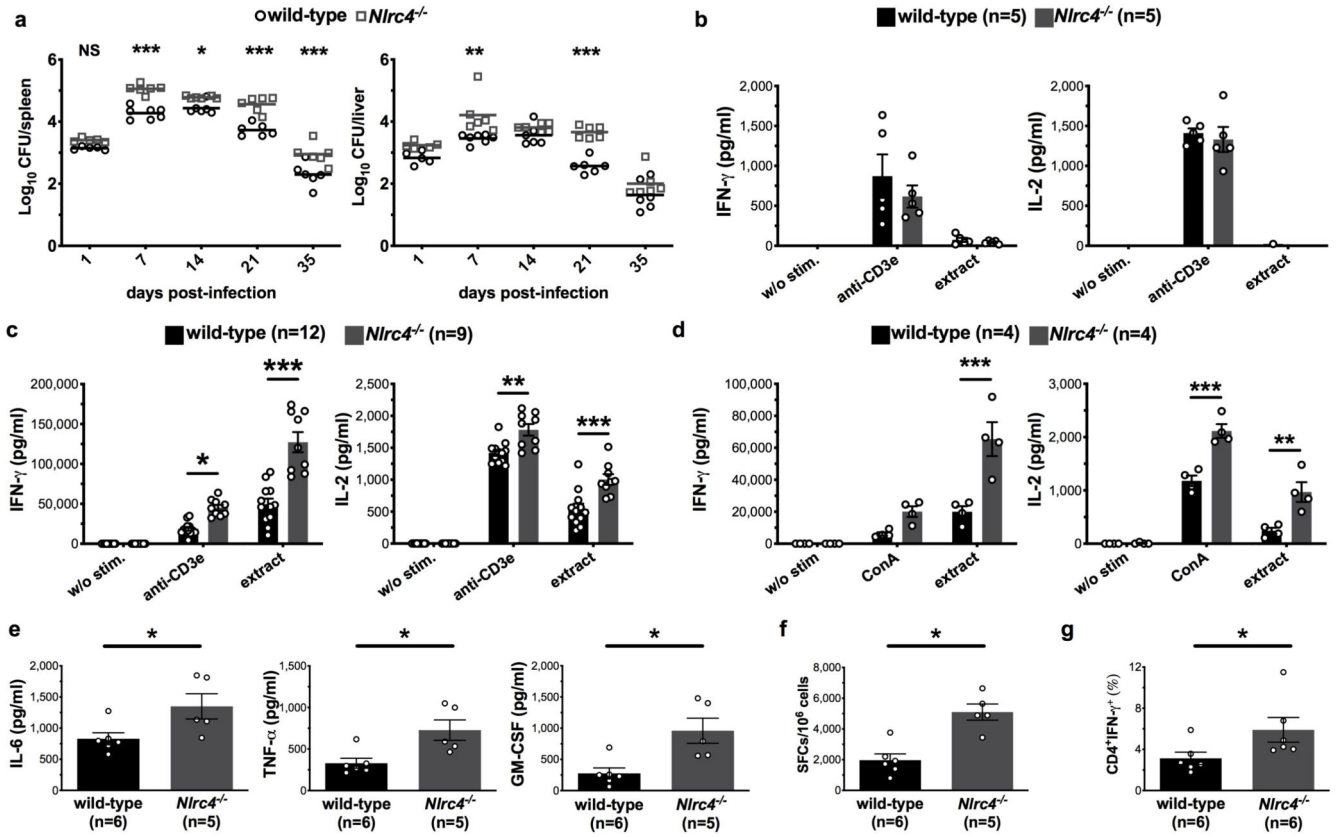
Figure 1. NLRC4 restricts bacterial spread in vivo and Th1 CD4$^+$ T cell-mediated memory responses *ex vivo*

a, Wild type and *Nlrc4$^{-/-}$* mice were challenged i.v. with 9.5x10^3 CFU *S.* Typhimurium M525P and microbial burden was determined in the spleen and liver at day 1 (n=5 for wild-type and *nlrc4$^{-/-}$*), 7 (n=7 for wild-type and n=6 for *nlrc4$^{-/-}$*), 14, 21 and 35 (n=6 for wild-type and *Nlrc4$^{-/-}$*) post-challenge. **b**, CD4$^+$ T cells from naïve wild-type and *Nlrc4$^{-/-}$* mice were stimulated *ex vivo* with medium only (w/o stim.), anti-mouse CD3e (anti-CD3e) or whole bacterial cell extract (extract). Levels of IFN-γ and IL-2 were measured by ELISA in the cell culture supernatant after 72 and 24 hours, respectively. **c**, CD4$^+$ T cells from wild-type and *Nlrc4$^{-/-}$* mice 90 days after challenge with 7x10^3-1x10^4 CFU of *S.* Typhimurium M525P were stimulated and levels of IFN-γ and IL-2 were measured as in **b. d**, CD4$^+$ T cells from wild-type and *Nlrc4$^-$* mice 168 days after challenge with 1.15x10^3 CFU of *S.* Typhimurium M525P were stimulated as in **b**, with the exception that concanavalin A (conA) was used instead of anti-mouse CD3e, and levels of IFN-γ and IL-2 were measured as in **b. e**, CD4$^+$ T cells from wild-type and *Nlrc4$^{-/-}$* mice 90 days after challenge with 7x10^3 CFU of *S.* Typhimurium M525P were stimulated with whole bacterial cell extract and levels of IL-6, TNF-α and GM-CSF were measured by fluorescent bead immunoassay in the cell culture supernatant after 24h. **f**, Same experiment as **e**, the number of CD4$^+$ T cells secreting IFN-γ in response to whole bacterial cell extract was measured via ELISPOT. **g**, Wild type and *Nlrc4$^{-/-}$* mice were challenged i.v. with 1.72x10^4 CFU and 112 days later, the percentage of CD4$^+$ T cells secreting IFN-γ in response to whole bacterial cell extract was measured via a cytokine secretion assay. Each symbol represents one mouse with horizontal lines delineate

the mean in a. Data are shown as mean ± SEM in b-g. Data are pooled from two and representative of at least four independent experiments for c and representative of three for a and two for **b**, **d, e, f** and **g** independent experiments. Statistical significance was calculated by 2-way ANOVA followed by Sidak's multiple comparisons tests for a-d and two-tailed Mann Whitney test for **e-g**.
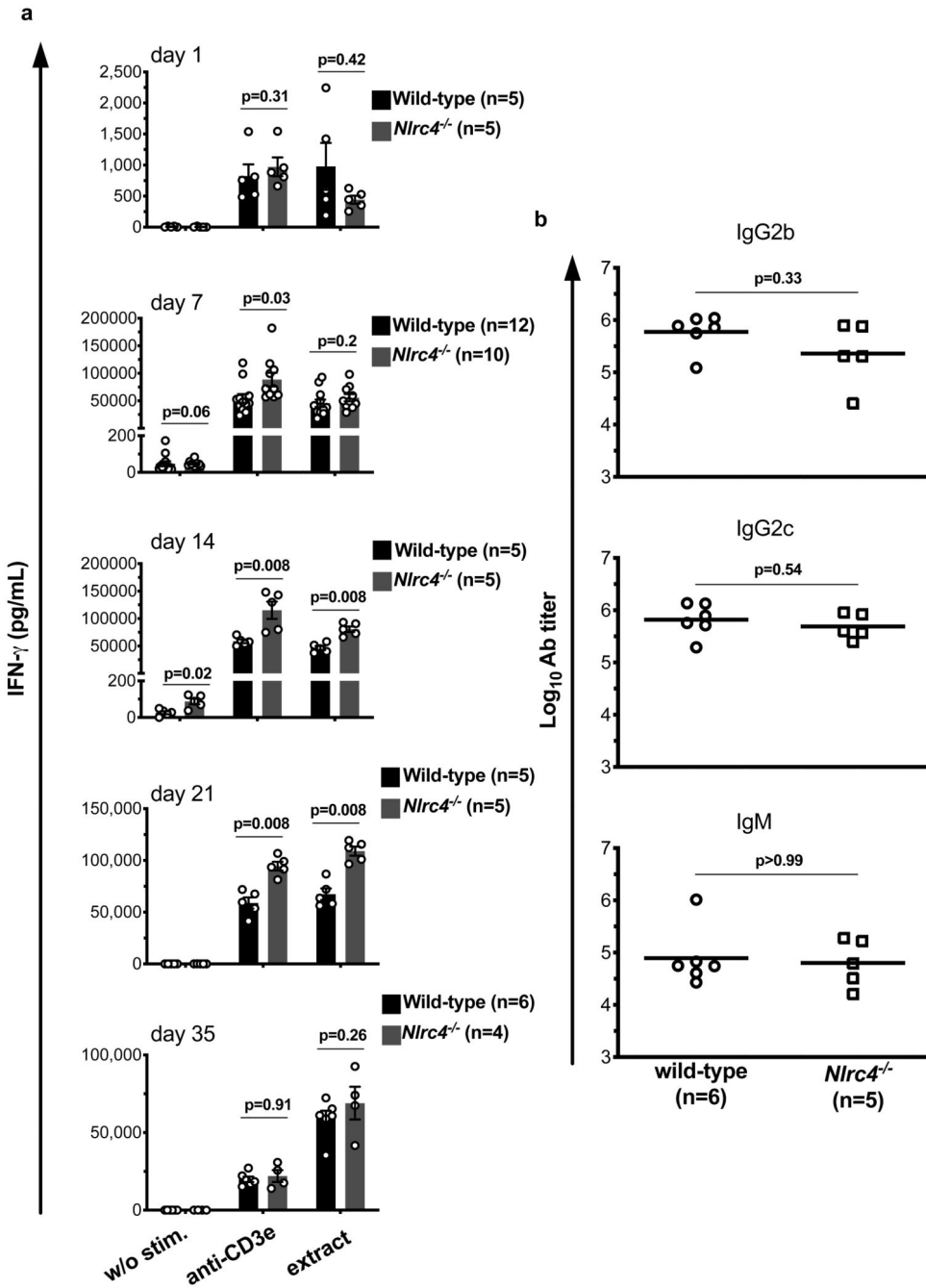
Figure 2. NLRC4 restricts the magnitude of effector CD4+ T cell responses during microbial clearance of a primary infection

a, Wild-type and *Nlrc4*-/- mice were challenged i.v. with 7.2×10^3-1×10^4 CFU of *S.* Typhimurium M525P and T cell-mediated responses were analysed over time. CD4+ T cells were co-cultured *ex vivo* with feeder cells in the presence of medium only (w/o stim.), anti-mouse CD3e (anti-CD3e), or whole bacterial cell extract (extract) and IFN-γ was measured by ELISA in the cell culture supernatant after 72 hours. **b,** Wild-type and *Nlrc4*-/- mice were challenged i.v. with 7×10^3 CFU *S.* Typhimurium M525P and levels of IgG2b, IgG2c and IgM antibodies against *S.* Typhimurium LPS were measured in the serum at 90 days post-

challenge via ELISA. Data are shown as mean ± SEM in **a**. Each symbol represents one mouse with horizontal lines delineate the mean in **b**. Statistical significance was assessed by two-tailed Mann Whitney test. Data are pooled from 2 independent experiments for **a**: day 7 and generated from one experiment in **a**: day 1, 14, 21 and 35. Data are representative of two independent experiments for **b**.
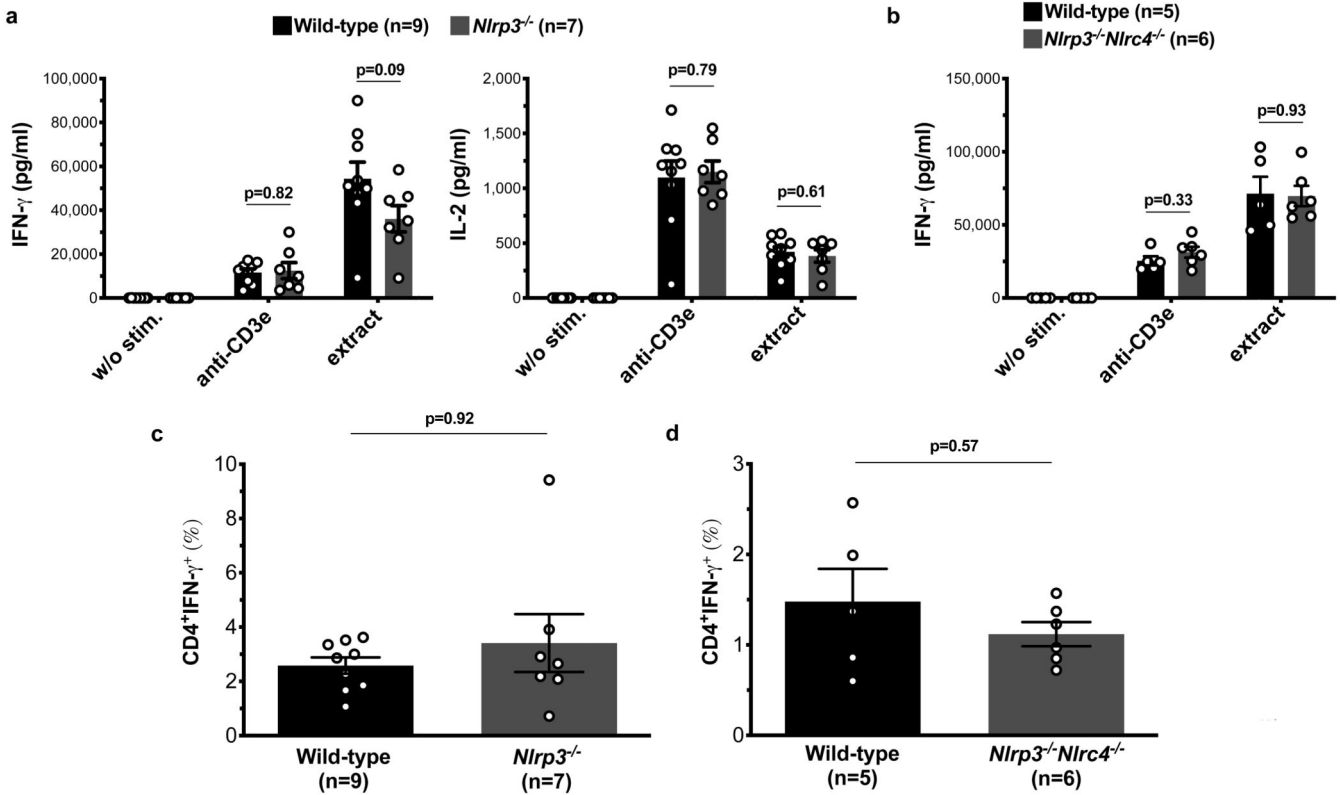
Figure 3. NLRC4 restricts the potency of CD4+ T cell-mediated memory responses against *Salmonella* in a NLRP3-dependent manner.

The Th1 memory response was assessed by stimulating CD4+ T cells *ex vivo* with medium only (w/o stim.), anti-mouse CD3e (anti-CD3e), or whole bacterial cell extract (extract). **a**, CD4+ T cells from wild-type and *Nlrp3-/-* mice 100 days after challenge with 2.2×10^4 CFU *S.* Typhimurium M525P and IFN-γ and IL-2 were measured by ELISA in the cell culture supernatant after 72 and 24 hours, respectively. **b**, CD4+ T cells from wild-type and *Nlrp3-/- Nlrc4-/-* mice 90 days after challenge with 1.72×10^4 CFU *S.* Typhimurium M525P and IFN-γ was measured as in **a. c** and **d**, same experiments as **a** and **b**, respectively, the percentage of CD4+ T cells secreting IFN-γ was measured via a cytokine secretion assay. Data are shown as mean ± SEM. Statistical significance was calculated using two-tailed, unpaired Student's t test assuming equal variances for **a** and **c** and two-tailed Mann Whitney test for **b** and **d**. All data are representative of two independent experiments.
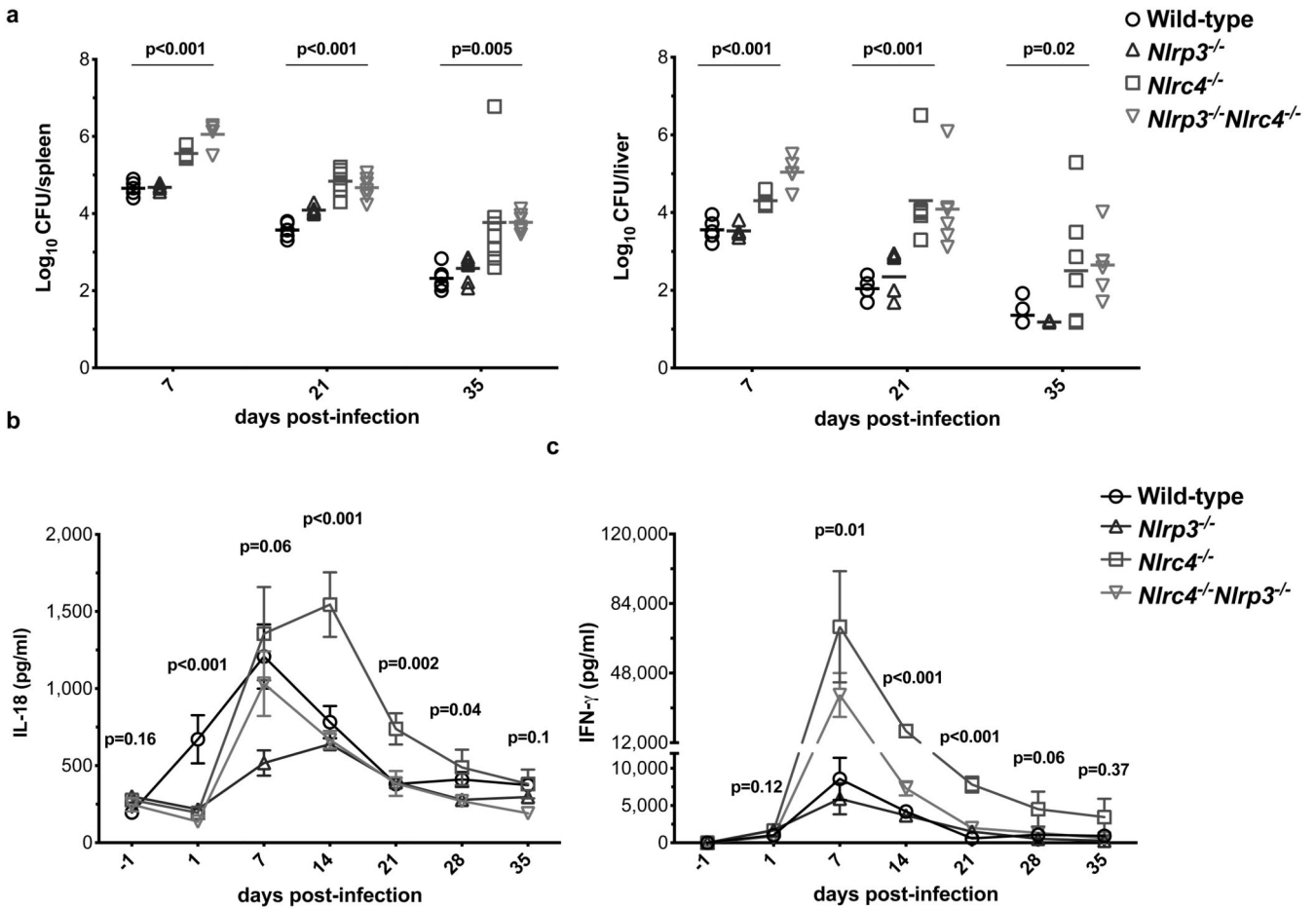
Figure 4. NLRC4 restricts NLRP3-dependent secretion of IL-18 and IFN-γ.

Wild type, *Nlrp3*^{-/-}, *Nlrc4*^{-/-} and *Nlrp3*^{-/-}*Nlrc4*^{-/-} mice were challenged i.v. with 1.86×10^4 CFU *S.* Typhimurium M525P. **a**, Bacteria were counted in the spleen and the liver at day 7 (n=5 for wild-type, *Nlrp3*^{-/-} and *Nlrp3*^{-/-}*Nlrc4*^{-/-} and n=4 for *Nlrc4*^{-/-}), 21 (n=6 for all genotypes) and 35 (n=6 for wild-type, *Nlrp3*^{-/-} and *Nlrp3*^{-/-}*Nlrc4*^{-/-} and n=7 for *Nlrc4*^{-/-}) post-challenge. **b**, IL-18 was measured in the serum at day 1 pre-challenge (n=5 for wild-type and *Nlrp3*^{-/-}*Nlrc4*^{-/-}, n=4 for *Nlrp3*^{-/-} and n=6 for *Nlrc4*^{-/-}) and day 1 (n=5 for wild-type and n=6 for all other genotypes), 7 (n=5 for wild-type, *Nlrp3*^{-/-} and *Nlrp3*^{-/-}*Nlrc4*^{-/-} and n=4 for *Nlrc4*^{-/-}), 14 (n=6 for wild-type and n=5 for all other genotypes), 21 (n=6 for all genotypes), 28 (n=6 for wild-type, *Nlrp3*^{-/-} and *Nlrp3*^{-/-}*Nlrc4*^{-/-} and n=5 for *Nlrc4*^{-/-}) and 35 (n=6 for wild-type, *Nlrp3*^{-/-} and *Nlrp3*^{-/-}*Nlrc4*^{-/-} and n=7 for *Nlrc4*^{-/-}) post-challenge by ELISA. **c**, IFN-γ was measured by fluorescent bead immunoassay in the serum over time with the same number of mice as in **b** apart from day 1 pre-challenge (n=5 for wild-type and n=4 for all other genotypes). Each symbol represents one mouse with horizontal lines delineate the mean in **a**. Data are shown as mean ± SEM in **b-c**. Overall statistical significancehas been determined by one-way ANOVA for each interval separately. For wild-type versus Nlrc4^{-/-}mice, data are representative of three independent experiments. For wild-type versus *Nlrp3*^{-/-} and *Nlrp3*^{-/-}*Nlrc4*^{-/-} mice, data are representative of two independent experiments.
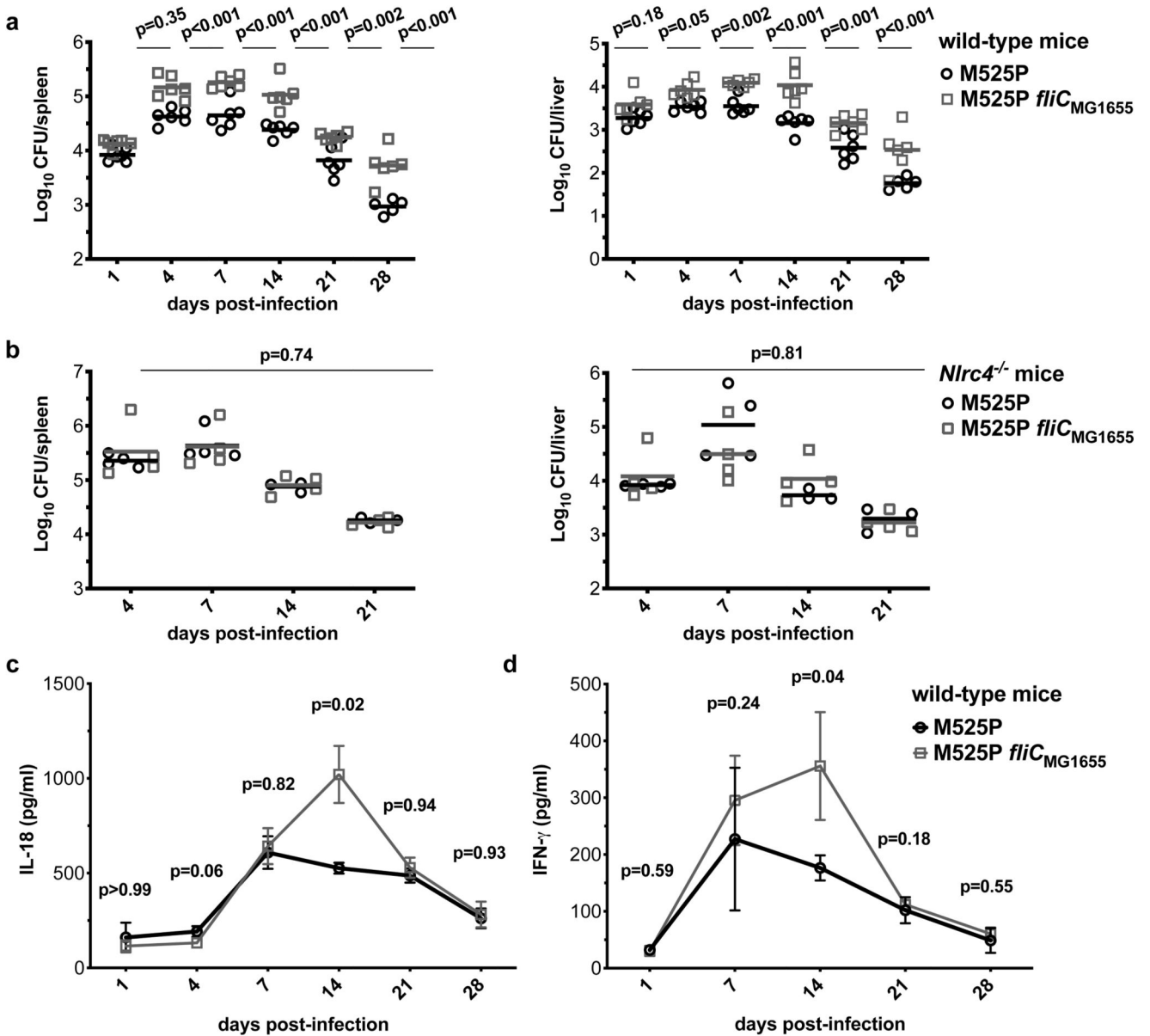
Figure 5. *Salmonella* expressing flagellin from non-pathogenic *E. coli* largely escapes NLRC4-mediated detection *in vivo*

Wild type and *Nlrc4^{-/-}* mice were challenged i.v. with 1.5×10^4 CFU *S.* Typhimurium M525P or M525P fliC$_{MG1655}$. **a,** Bacteria were counted in the spleen and the liver of wild-type mice over time (n=6 for both groups for all days apart from day 35; n=5 for M525P and n=6 for M525P *fliC*$_{MG1655}$). **b,** Bacteria were counted in the spleen and the liver of *Nlrc4^{-/-}* mice over time (day 4 and 7; n=4 for both groups, day 14 and 28; n=3 for M525P and n=4 for M525P *fliC*$_{MG1655}$). **c,** IL-18 was measured in the serum of wild-type mice over time by ELISA with the same number of mice as in **a**. **d,** IFN-γ was measured in the serum of wild-type mice over time by a fluorescent bead immunoassay with the same number of mice as in **a**. Each symbol represents one mouse with horizontal lines delineate the mean in **a-b**. Data are shown as mean ± SEM in **c-d**. Statistical significance was calculated by 2-way ANOVA

followed by Sidak's multiple comparisons tests in **a** and **b** and two-tailed Mann Whitney test for each time point separately in **c** and **d**. All data are representative of two independent experiments.
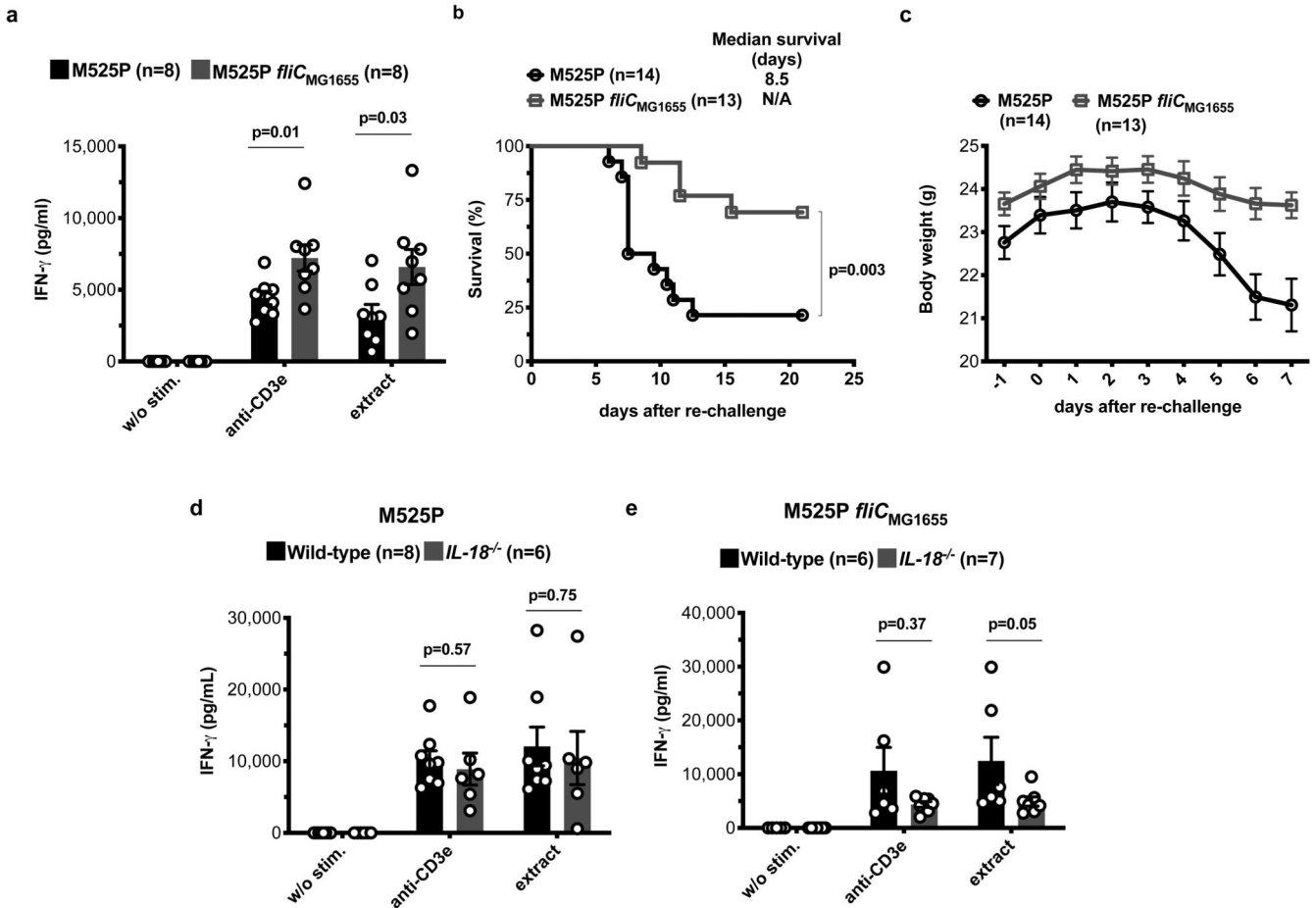
Figure 6. Primary challenge with *Salmonella* expressing flagellili from nonpathogenic *E. coli* improves protection against lethal re-challenge

a, CD4+ T cells from wild-type mice 122 days after challenge with 1.5×10^4 CFU *S.* Typhimurium M525P or M525P *fliC*$_{MG1655}$ were stimulated with medium only (w/o stim.), anti-mouse CD3e (anti-CD3e), or whole bacterial cell extract (extract). IFN-γ was measured by ELISA in the cell culture supernatant after 24 hours. **b,** Wild-type mice were challenged with 1.6×10^4 CFU *S.* Typhimurium M525P or 1.5×10^4 CFU M525P *fliC*$_{MG1655}$ and allowed to clear the primary infection for 128 days. They were then re-challenged orally with 4.8×10^6 CFU *S.* Typhimurium SL1344 and euthanized upon detection of adverse signs. **c,** In the same experiment as in **b**, mouse weight was recorded at least once daily and shown for the first seven days of infection. **d**, CD4+ T cells obtained from wild-type and *IL-18*$^{-/-}$ mice 104 days after primary challenge with 1.6×10^4 CFU *S.* Typhimurium M525P were stimulated and IFN-γ was measured as in **a. e**, CD4+ T cells obtained from wild-type and *IL-18*$^{-/-}$ mice 110 days after primary challenge with 3.3×10^4 CFU *S.* Typhimurium M525P *fliC*$_{MG1655}$ were stimulated and IFN-γ was measured as in **a**. Data are shown as mean ± SEM in **a**, **c**, **d and e** and as a survival curve in **b**. Statistical significance was calculated by a two-tailed Mann Whitney test in **a**, **d** and **e** and two-sided log-rank in **b**. Data are

representative of two independent experiments for a and were generated from one experiment for **b-e**.